Towards Semantic-Empowered Communication

Shirin Rezasoltani

A Thesis

in

The Department

of

Electrical and Computer Engineering

Presented in Partial Fulfillment of the Requirements for the Degree of

Master of Applied Science (Electrical and Computer Engineering) at

Concordia University

Montréal, Québec, Canada

August 2021

CONCORDIA UNIVERSITY

School of Graduate Studies

This is to certify that the thesis prepared

By: Shirin Rezasoltani

Entitled: **Towards Semantic-Empowered Communication**

and submitted in partial fulfillment of the requirements for the degree of

Master of Applied Science (Electrical and Computer Engineering)

complies with the regulations of this University and meets the accepted standards with respect to originality and quality.

Signed by the Final Examining Committee:

______________________________ Chair
Dr. Dongyu Qiu

______________________________ Examiner
Dr. M.K. Mehmet Ali

______________________________ Examiner
Dr. Dongyu Qiu

______________________________ Supervisor
Dr. Chadi Assi (CIISE)

______________________________ Co-supervisor
Dr. Leszek Szczecinski (INRS)

Approved by ______________________________
Dr. Y.R. Shayan, Chair
Department of Electrical and Computer Engineering

______________ 2021

____
Dr. Mourad Debbabi, Dean,
Gina Cody School of Engineering and Computer Science

Abstract

Towards Semantic-Empowered Communication

Shirin Rezasoltani

The issues of timeliness and accuracy are becoming increasingly important with the advent of heterogeneous applications/networks and standardization of new services in areas of Cyber-Physical systems where the popular performance measures such as the throughput, error rate and packet loss lose their intuitive interpretation and new formal metrics must be defined on which the intuition will be built. To solve this problem, Semantic of Information has been recently introduced: the purpose and the final utility of the delivered data should be considered, and the performance is to be related to the semantics.

In this thesis, we explore two major issues in the area of semantic communications. First, we investigate the issue of wireless sensing in non-real time systems when the time delivery constraints are not restricted to be in real domain and the system tolerates delay in accessing the measurement results. To illustrate the application of this principle, we use the Markovian Gaussian models, and assuming the information semantic, we study the optimal estimation methods to non-causally reconstruct the source signal. We derive the explicit expressions and optimal buffer management policies for the proposed information accuracy metric.

Second, we evaluate the impact of the erroneous wireless control feedback channel using the Age of Information, one particular metric for semantic communications to capture the freshness and timeliness of information in real-time applications. To mitigate the impact of the imperfect feedback channel on the system performance, we adopt a Binary Asymmetric Channel model to control the detection accuracy of the control signals. We then compute the explicit expressions for the average Age of Information. Further, we show the optimum parameter design for the control channel model in order to minimize the average Age of Information.

Acknowledgments

It is a genuine pleasure to express my sincere gratitude to my thesis advisors Dr. Chadi Assi for his continuous support of my research. I am thankful to him for giving me this opportunity to work and study under his guidance.

My sincere thanks also goes to my co-supervisor, Dr. Leszek Szczecinski for his continuous supervision, prompt and useful advice, and insight comments to better this research.

Besides, I am extremely thankful to my fellow lab mates for their friendship, kind help and all the invaluable support they showed me through these years.

Last, but definitely not the least, I would like to thank my parents and my sister for their constant supports throughout my life. Without their love and support, I could not overcome the difficulties during these years.

Contents

List of Figures

Abbreviations

AAoI	Average Age of Information
ACK	Acknowledgement
AMC	Adaptive Modulation and Coding
AoI	Age of Information
AR(1)	Autoregressive Process(1)
ARQ	Automatic Repeat reQuest
BAC	Binary Asymmetric Channel
HARQ	Hybrid Automatic Repeat reQuest
i.i.d.	independent, identically distributed
MDP	Markov Decision Process
ML	maximum likelihood
NACK	Negative Acknowledgment
PMF	Probability Mass Function
SNR	Signal to Noise Ratio
SoI	Semantic of Information

List of Symbols

Semantic Communications for Non-Real Time Applications

λ	Packet arrival rate at the sensor
ε	Parameter of decoding failure probability in ARQ scheme
θ	Parameter of decoding failure probability in HARQ scheme
ϕ	SNR of the forward channel
snr	Average SNR of the forward channel
κ	Parameter of AR(1) process
Υ	Causal estimation error
υ	Non-causal estimation error
δ	Information lag
Δ	Age of Information
X	Inter-generation time of the successfully delivered packets at the monitor
I	Waiting time to recieve a sample at the sensor
F	Time duration server busy with transmission of consecutive preempted packets
Y	Service time of a successfully delivered packet at the monitor
R	Inter-generation time of arrived packets at the sensor
S	Service time of a packet
a	Action

π Policy set

η Discount factor

ξ Relative excess average non-causal error

Ξ Relative excess average causal error

Real Time Status Updates in Wireless HARQ with Imperfect Feedback Channel

λ Packet arrival rate at the sensor

snr_c Average SNR of the forward channel

snr_d Average SNR of the feedback channel

ε Parameter of decoding failure probability in ARQ scheme

θ Parameter of decoding failure probability in HARQ scheme

Θ Threshold in BAC model

Θ^* Optimal value of threshold in BAC model

ε_A Probability of ACK miss-classification as NACK

ε_N Probability of NACK miss-classification as ACK

ρ Nominal transmission rate

Δ Age of Information

$\overline{\Delta}_*$ Optimum value of Age of Information

X Inter-departure time of the successfully delivered packets at the monitor

I Waiting time to receive a sample at the sensor

Y Service time of a successfully delivered packet at the monitor

Δ_∞ Age of Information in a perfect error-free feedback channel

Notations

$\lvert . \rvert$	Absolute value
σ^2	Variance of normal distribution
$\mathcal{N}\left(0, \sigma^2\right)$	Normal distribution with zero mean and variance σ^2
$\mathbb{E}(\cdot)$	Expected value
$\mathbb{1}(\cdot)$	Indicator function
$\gamma(\theta, k)$	Lower incomplete Gamma function
$G(\cdot)$	Probability generating function
$Q(\cdot)$	Q-function

Chapter 1

Introduction

1.1 Overview and Motivation

In recent years, researchers have altered their visions toward 6G and networks beyond 5G to support the development of new applications and communication systems. The tremendous growth and advances in the area of intelligent control systems and its various fields, including smart transportation and manufacturing facilities, intelligent traffic control, etc., have all exposed limitations in the applicability of the traditional sensing and communication techniques [1–3]. In such systems, “timely access" to “accurate information" from the environment plays a major role in guaranteeing the performance and efficiency of these intelligent systems.

Typically, a traditional remote estimation system contains different blocks including sensing (data acquisition from the environment), communication (data delivery to the destination) and application (data estimation to monitor or control). Conventionally, the overall system design is independent of the ultimate usage of the individual information packet at the application level. More precisely, the traditional architecture treats the same with all the generated packets at the sensing layer, and thus the communication part targets to deliver reliably every arrived packet to the destination. In this regard, different performance metrics such as throughput, delay and packet loss have been widely applied to design the system in the past decades. For instance, 4G applications demand for high throughput while Ultra Reliable Low Latency (URLLC) systems require high reliable throughput with low latency.

As we noticed, the architecture of these systems are oblivious to the importance, meaning and final utility of the data packets at the receiver since the whole set of generated packets are important to be delivered reliably to the receiver. Every packet that either lost or delivered late will impose a reduction in the system performance and reduce the overall Quality of Service (QoS). Due to this behavior, the current communication systems are content-blind [4]. The fact that elements such as time, space and application may affect and change the importance and meaning of the data packet is completely abandoned in the current and traditional system designs. However, a class of new emerging applications require a content-based communication system in which the packets transfer according to their final usage in the system. The service quality of new emerging applications in the area of Internet of Things (IoT) mainly depends on timely generation and delivery of meaningful, accurate and valid information packets.

In new content-based applications [4], applying the traditional architecture of the communication systems will lead to QoS dissatisfaction as well as to network bottlenecks. First off, not all packets delivered at the destination are useful in the application layer. Precisely, trying to deliver all generated packets and increasing throughput or reliability of the system will cause to transmission of out-dated and useless information to the destination. Besides, reducing the delay of the transmission process of the whole set of generated information will not guarantee the on-time delivery of the set of meaningful and valid information in the destination. Second, since the destination only requires the set of meaningful, accurate and fresh data packets, a system defined with traditional performance criteria, such as throughput will only yield to network bottlenecks. Given the tremendous growth of number of connected devices in IoT networks, we can anticipate huge network traffic. Clearly, an optimal and structural system design based on the final application demand can reduce the traffic and avoid bottlenecks in network.

Recently, the Semantic Communications [4, 5] has been introduced to remove the boundaries of the traditional communication systems and to redesign the existing practical architectures and infrastructures. Very fundamental consideration for these networks is the tight connection between the entire three processes of sampling, transmission and reconstruction which must be performed with regard to the perfectly formulated performance metrics, see Fig. 1.1. In this way, the traffic load of the uninformative information packets will be eliminated and resources would be occupied

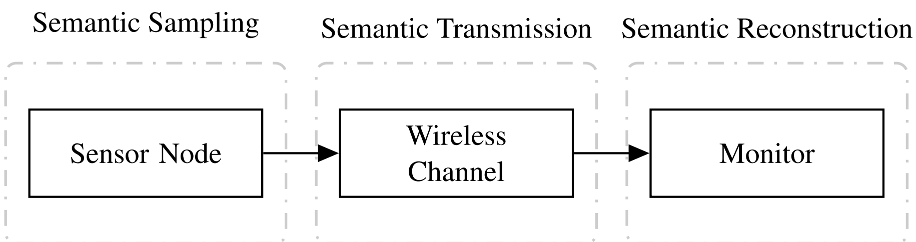

Figure 1.1: Architecture of Semantic Communication

more efficient.

While undoubtedly, the “performance" and “efficiency" of the discussed emerging applications depend on the “timely" access to “accurate" information obtained from the source, the very concepts of timeliness and accuracy become intertwined and thus defining the performance criteria for evaluation and/or design may be difficult. To address this problem, the purpose and the final usage of the delivered data should be considered, and the performance is to be related to the ultimate usage of the transmitted information, e.g., [4]. During the recent years, different performance criteria have been introduced in the literature to model the performance of these new systems and measure the semantics. Accordingly, we may name these metrics Semantic of Information (SoI) [5]. We can categorize the SoI metrics in three levels as presented in the following.

At the first level of approximation, the semantics may be defined through a distortion of the sensed signal contained in the transmitted messages and reconstructed at the monitor. This approach was adopted in [6], and while this perspective does not capture the ultimate utility of the information (e.g., for control or for decision making), it already allows us to go beyond the limitations of the conventional approach, which only focused on delivering reliably the messages without questioning their contents. Important to note is that, to evaluate the distortion, we have to make assumptions regarding the model of the signal. In addition, considering the distortion function as the performance criteria will result into a co-design of all the three process of sampling, transmission and reconstruction.

Secondly, to tackle the semantics *without* specifying the model of the signal, we may look at certain parameters of the transmission which are deemed as important. In particular, the recent years witnessed the explosion of interest in the Age of Information (AoI). Defined at time t as $\Delta_t = t - t_{-}$, where t_- is the time-stamp of the most recent sample available at the time t, the AoI has an appealing simplicity and the intuitive interpretation of "timeliness" or "freshness" of information.

In addition to the capability of AoI in modeling data freshness, this metric can be interpreted as the level of dissatisfaction for having a stale data at the destination. Depending on the application demand, a various class of AoI based metrics have been defined and analysed in some recent works which are basically the non-linear transformations of AoI [7], [8], [9]. Ideally, if the status of the sensor node could be delivered at the remote monitor at every time slot without delay, the AoI will stay at its minimum level, and the information available at the destination is always fresh. However, the wireless networks inherently suffer from the random delays in the wireless channel as well as the sampling process. Therefore, it is necessary to design optimally the whole communication system with regard to the AoI metric to keep the monitor at the desired level of information freshness.

At last, a multi-variable function of timeliness and estimation accuracy has been studied in some recent works [4]. Some other transformation functions of timeliness and accuracy are defined in [10, 11]. Basically, the amount of time that the estimation error is violating a pre-defined level is questioned in these works.

The research on the Semantic of Information and Communication Semantics is still in its very early stages and different questions and problems are still needed to be discovered and addressed.

1.2 Problem Statement

In this thesis, we focus our efforts on defining two major issues and proposing frameworks to study and analyse them.

The first chapter of the work challenge the assumption of limiting the semantic applications to only real-time scenarios. Fundamental for all the previous works on the semantics is the assumption of real-time applications being served, where the delay is intuitively the critical criterion. However, given that the entire discussion about the semantics of information is carried out in the context of heterogeneity of applications, it is entirely natural to question this real-time requirements, as also noted in [4, Sec. II.B]. Of course, the requirements in the case of non-real time applications will be *different* from the real-time case, but we still need to quantify/estimate these requirements.

In the previous chapter, we assume an erroneous wireless forward channel and an error free wireless feedback channel. However, we know that a practical wireless system suffers from the errors in both forward and backward channels. In the second chapter of the thesis, we address the aforementioned issue of unreliability in both forward and backward wireless channels in a semantic communication system in which the semantics are measured and quantified through the recently introduced metric AoI. In the recent works studying the effect of different re-transmission strategies on the performance of AoI, e.g., [12, 13], one major assumption is the existence of a noiseless feedback channel so that the decoding success or failure will be perfectly known at the sensor. Such assumption may not fully capture the behaviour of the system in real practical settings since the wireless feedback may, as well, be unreliable and noisy. Most importantly, industrial controlling applications are prone to errors in the control feedback link, which is a direct result of the power limitations and interference introduced from a dense network of users.

In traditional telecommunication as well as wireless networks [14], however, errors in the feedback channel can lead to miss-detection and hence erroneous decoding result. Therefore, packet re-transmission decisions at the sensor side may yield an inefficient performance which lowers the system throughput and increases the delay in packet delivery procedure. Clearly, assuming a perfect error-free feedback channel is not practical and the results obtain from such analysis may mislead to a wrong real-time system design. Consequently, we study the system performance in terms of AoI metric, in addition, an optimal system design are presented to mitigate the impact of error in wireless channels.

1.3 Related Works

Recently, the authors of [4, 5] introduced the notion of information semantic as a new concept which can meaningfully construct the basis for the architectural design of emerging communication systems. Considering that in a sensor communication network, information value can change with the provided level of accuracy within time [4], we can classify the recent literature on information semantics mainly into three folds.

The first venue addresses directly the issues of the source model, of the estimation strategy, as well as of defining the distortion metric. It should be seen as a generalization of the approach underlying the definition of the AoI (where the signal is modeled as a Wiener process, the estimation is done by a causal zero-order linear interpolation, and the distortion is defined by variance of the estimation error). In particular, [7] and [15] studied the auto-correlation and mutual information functions between the current time estimation and the actual state of the source to characterize the real time estimation of the signal. The discrete model of the source was analyzed in [16]. The authors in [17] considered the source to be a Poisson counting process and defined the related distortion function. The same methodology is applied for OU process in [18] which should be seen as application of the principle of the causal estimation [19] to the colored Gaussian noise model.

In the second cluster of work, the performance criteria is modified and the combination of time-based and error-based metrics to evaluate the information semantic are formulated. Some recent works in this venue introduced new metrics such as Value of Information [20], Age of Incorrect Information [10] and Urgency of Information [11]. Similarly, the non-linear transformations of the AoI were proposed in [21,22].

The last venue borrows the definition of AoI to analyse how the timeliness depends on the sampling methods [19], transmission schemes and channel models [12,23–25], buffer management strategies [26,27]. Some other works focus on a statistical analysis of the AoI random process itself by finding the metrics which go beyond the long term average. In particular, the distribution of the AoI was found in [26], while the distribution of the AoI peak was studied in [28].

Since the introduction of real time systems and AoI metric, much work has been conducted to study the effect of diverse aspects of system elements on the AoI. Some prior work focused on the sensor buffer capacities and studied the queuing of update packets [19]. While other works analysed different queue management policies to deliver updates in minimum AAoI, i.e., [29–31].

Some other recent works, e.g., [12,13,32], focused their efforts to take into account more practical and real assumptions about the communication channel between the sensor and the monitor. The authors of [12] and [13] used predefined functions to determine the decoding errors; while they qualitatively describe the actual HARQ decoding, they rely on neither the model of the channel nor the decoding principles. To gain insights into the behaviour of AoI in wireless HARQ the canonical models of wireless communications are used in [23], where the block fading channel was used to analyze AoI for different re-transmission schemes.

The impact of noisy feedback channel on the packet transmissions has been studied before in some previous works [33–35]. The performance criteria assumed in this class of works was mostly the long-term throughput [36] and the system reliability in terms of packet loss rate [37]. The truncated versions of re-transmission schemes has been studied in papers such as [38] and [39]. Authors in some other works studied the noisy feedback channel for more specific communication system setups like LTE communication systems in [40] or CDMA systems in [41].

1.4 Outline and Contributions

This dissertation includes two chapters. In the first part of the work, We discuss the concept of SoI in terms of distortion function for the non-real time application. We argue, that in the wireless transmission with simple transmitters, e.g., in wireless sensor networks, the quality of signal reconstruction at the transmitter is affected by the channel and the adopted transmission strategies even if the reconstruction is carried out non-causally. Using the ideas applied previously in the context of real-time application, we define the non-causal distortion function for Markovian Gaussian models at the source. Moreover, we derive the formulas for the long-term average of newly defined metric for two buffer management strategies and we show the results of optimal buffer management obtained from the Markov Decision Process (MDP) formulation. Numerical examples based on the above formulas and results are shown to illustrate the fact that the transmission strategies derived for real-time application lose their optimally when the non-causal reconstruction at the monitor is considered.

The second part of the work designs a practical communication system by assuming a model for the feedback control channel. Precisely, We employ a Binary Asymmetric Channel (BAC) model in the sensor side to detect the received signal and classify it as either ACK or NACK message. Since ACK and NACK error detection each may play different roles in the ultimate AoI value, such a BAC setup can properly control the destructive effects the wrong detection may cause on the age function. Then, we derive the closed-form expressions of AAoI for preemptive and non-preemptive queue policies with respect to the error models of forward and feedback channels. The theoretical results are general that can be quickly applied for any binary classification method, including BAC model, that is used to detect the errors in the feedback channel. Moreover, we explore the optimum parameter setups in BAC model design to minimize the destructive impact of ACK/NACK unreliability on the AoI performance and to achieve the minimum average AoI value. Further analysis reveals that the conclusions about the usefulness of a particular re-transmission scheme may change depending on the reliability of the acknowledgment detection at the sensor and the reliability of the forward channel. Results also unveil that the optimal BAC model for preemptive queue tends to re-transmit packets blindly in order to mitigate the destructive effect of the erroneous feedback messages on the AoI. However, the cost of blind re-transmission is increasing the unnecessary utilization of the channel resources. To show such a trade-off between the AoI performance and the occupied resources, we introduce and compute the average resource utilization in both ARQ and HARQ schemes. Moreover, we show how the optimum BAC design for a non-preemptive queue is affected by the status arrival process.

The remainder of this dissertation is organized as follows: In chapter 2, we introduce the SoI metric along with the long term average metrics for a non-real time system. Then, we derive the explicit equations for fixed queue policies as well as the optimal queue policies considering two types of packet re-transmission schemes. In chapter 3, we formulate a wireless communication system with noisy forward and feedback channels, and present a general framework to analyse the impact of erroneous channels on the metric AoI as well as the channel occupancy. In chapter 3, we present all the conclusions and possible future research works.

Chapter 2

Semantic Communications for Non-Real Time Applications

This chapter investigates the semantic communications [5, 42] in wireless sensing systems, particularly those used by non-real time applications.

To define the performance criteria, we turn again to the concept of semantics, where the main difference with the real-time applications is that we may use non-causal reconstruction strategy. In fact, from the modelling perspective, this is the only difference and, depending on whether we want to use explicitly the model of the source or not, we will obtain different definitions of semantic of information proper to the context of non-real time applications. This is a simple approach to generalize the concepts used previously solely in the real-time context.

Similarly to the real-time applications, non-real time systems still suffer from the random delay, the packet loss and all others impairments of the communication systems. We might argue, of course, that non-real time applications may benefit from the retransmissions so that, ultimately, no packet loss is incurred. However, such an argument, valid in general, ignores the fact that the remote sensing will (possibly) use simple sensors which cannot backlog the information. Thus, while we can tolerate the delay to gather all the required information to begin the reconstruction, we are still required to design efficiently every part of the communication system including the buffer controller, the transmission strategy as well as the estimation methods at the monitor.

We apply the introduced framework over the Markovian Gaussian models and, assuming the noisy wireless channel, we study the optimal estimation methods to non-causally reconstruct the source signals at the destination. Further, we derive the explicit expressions and optimal buffer management policies for the information accuracy defined as the distortion function. Lastly, we analyze the impact of the non-causal approach in the case of sub-optimal estimation method, a case which is practically relevant as well, because the parameter of the signal model is, in general, unknown at the monitor.

This chapter is organized as follows: In Sec. 2.1 we explain the system model. In Sec. 2.2 we define the distortion function for non-causal reconstruction. The packet management under fixed and optimum policies are studied in 2.3 and 2.4. Section 2.5 provides the analysis and illustrates it with numerical examples; conclusions are drawn in Sec. 2.6.

2.1 System model

We consider a problem where a *sensor* communicates measurements to a *monitor* through a wireless channel and receives the acknowledgments through an error-free feedback channel. We deal with discrete time slots of unit length where time slot $t = 0, 1, 2, \ldots$ corresponds to the time duration $[t, t+1)$.

Measurement signal: We must express our idea about the dynamics of the physical process being sensed, as well as define the sampling policy. Here, we assume the process follows either Wiener process or Ornstein-Uhlenbeck (OU) model:

- Wiener signal:

$$x_t = x_{t-1} + u_t, \tag{2.1}$$

- Ornstein-Uhlenbeck (OU) signal:

$$x_t = \kappa x_{t-1} + \sqrt{1-\kappa^2} u_t, \tag{2.2}$$

where x_t is the signal value at time t and u_t is a zero-mean, unit variance white Gaussian noise and $|\kappa| < 1$ has the meaning of the auto-correlation. The fundamental difference with the Wiener process is that the OU process is stationary (in particular, it has a finite variance) and thus may better model the the real-world signals.

We assume that the sampling of x_t is done independently in each time slot with probability λ, i.e., is Bernoulli distributed [12]. The inter-arrival time (the number of time frames between two updates at the sensor), R, follows then a geometric distribution[1]

$$R \sim \text{Geom}(\lambda). \tag{2.3}$$

Once the signal is sampled, it is embedded into a message that is passed to the sender.

Transmission channel: The message is encoded into a packet which is transmitted wirelessly. We adopt the canonical Rayleigh block fading model, i.e., the signal-to-noise ratio (SNR) in each slots, ϕ, varies randomly from slot-to-slot and is drawn from exponential distribution

$$p(\phi) = \frac{1}{\mathsf{snr}} \exp\Big(-\frac{\phi}{\mathsf{snr}}\Big), \tag{2.4}$$

where snr is the average SNR. We assume that the instantaneous SNR, ϕ, is unknown at the sensor (transmitter). Thus, the adaptation of modulation, coding or power is infeasible and the transmission is carried with the nominal rate ρ and unitary power. Consequently, the decoding errors are unavoidable and dealt with via retransmissions controlled by the feedback channel carrying the positive acknowledgment (ACK) or negative acknowledgment (NACK) messages. After receiving a NACK message in the round k, the event denoted by NACK_k, the sensor transmits again the same packet. The transmission stops after an ACK is received. For simplicity, the ACK and NACK messages are assumed to be delivered without errors and we consider the infinite HARQ.[2]

We consider two types of HARQ. The simplest case is ARQ, where in the k-th round, the monitor decodes the signal using the latest transmission outcome $\mathbf{y}_k$. In this case, we assume that the decoding error, NACK_k, occurs at round k, if the SNR, ϕ_k is below the decoding threshold define

[1]It should be interpreted as follows : if $R \sim \text{Geom}(\lambda)$ then $\Pr\{R = k\} = (1-\lambda)^{k-1}\lambda, k \geq 1$.

[2]In truncated HARQ, the number of rounds is limited but the analytical approach is simplified without such a constraint.

as follows

$$\{I(\phi_k) < \rho\} \implies \mathsf{NACK}_k, \tag{2.5}$$

where $I(\phi) = \log_2(1+\phi)$, that is we assume that the Shannon limit for the encoding-decoding scheme is attainable. This idealization is often used to analyze HARQ in block fading channel [43, 44] and then, the decoding errors are attributed to the random variation of the SNR.

If, on the other hand, the receiver is able to decode the information using all received signals $\mathbf{y}_1, \ldots, \mathbf{y}_k$, we deal with *repetition-redundancy* HARQ and then the packet combining produces the effect of SNR accumulation. Therefore, the decoding error condition is defined as [43, 44]

$$\Big\{I\big(\sum_{l=1}^{k} \phi_l\big) < \rho\Big\} \implies \mathsf{NACK}_k; \tag{2.6}$$

we will simply refer to it as HARQ.

The models in (2.5) and (2.6) affect the distribution of the service time, S, defined as the number of time frames required to deliver the packet, i.e., the number of frames necessary to receive the ACK. Knowing that $\Pr\{S = k\} = \Pr\{\mathsf{ACK}_k\} = \Pr\{\mathsf{NACK}_{k-1}\} - \Pr\{\mathsf{NACK}_k\}$, we need to find the $\Pr\{\mathsf{NACK}_k\}$ to define the service time distributions. From the exponential distribution of SNR and (2.5) and (2.6), we obtain the $\Pr\{\mathsf{NACK}_k\}$ for ARQ and HARQ as the following

$$\Pr\{\mathsf{NACK}_k\} = \begin{cases} \varepsilon^k & \text{ARQ} \\ \gamma(\theta, k) & \text{HARQ}, \end{cases} \tag{2.7}$$

where $\varepsilon = 1 - \mathrm{e}^{-\theta}$, $\theta = \frac{(2^\rho - 1)}{\mathsf{snr}}$ and $\gamma(\theta, k) = \int_k^\infty x^\theta \mathrm{e}^{-x} \mathrm{d}x$ is the lower incomplete gamma function. Finally, we obtain the following distribution for S,[3]

$$S \sim \begin{cases} \mathrm{Geom}(1-\varepsilon) & \text{ARQ} \\ \mathrm{Pois}(\theta) & \text{HARQ}, \end{cases} \tag{2.8}$$

[3]The distribution-based notation should be interpreted as follows : if $S \sim \mathrm{Geom}(\varepsilon)$ then $\Pr\{S = k\} = (1-\varepsilon)^{k-1}\varepsilon, k \geq 1$; and $S \sim \mathrm{Pois}(\theta)$ means $\Pr\{S = k\} = \frac{\theta^{(k-1)}}{(k-1)!}\mathrm{e}^{-\theta}, k \geq 1$.

with

$$\mathbb{E}[S] = \begin{cases} \frac{1}{1-\varepsilon} & \text{ARQ} \\ 1+\theta & \text{HARQ.} \end{cases} \tag{2.9}$$

Buffer management We will assume a single-packet buffer at the sensor where only two policies are possible: the *preemptive* one, where the packet under the service is dropped upon arrival of a new packet, and the *blocking* policy which drops the new packet if the transmission of the the previous one is not finished.

Estimation at the monitor After receiving the messages, the monitor must find the estimate $\hat{x}_t$ of the process being monitored. This is where the core problem lies because the estimation relies on the model of the process. We deal with this issue separately, in Sec. 2.2.

2.2 Semantic of information for non-real time applications

The semantic of information currently considered in the literature uses the AoI, [19] or its non-linear transformation, [45].

The most intuitive interpretation of the AoI as the "timelinesss" is well understood in the causal reconstruction context because the AoI actually measures the difference between the current time and the moment the most recent sample available at the monitor was generated at the sensor.

In this timeliness interpretation of the AoI little is presupposed about the signal. Nevertheless, we still tacitly assume that by measuring the lag from the most recent sample provides a sufficient insight into the estimation uncertainty. In other words, we suppose that knowing the last sample, we are not affected by its past. This Markovian model thus implicitly underlies the use of the AoI as a timeliness metrics.

Another interpretation is that of the estimation accuracy because the AoI is proportional to the variance of the estimation error under assumption of the source signal being a Wiener process [19] as in (2.1). In this sense, the Wiener process is a canonical model of the sensed signal.

On the other hand, by using non-linear transformations of the AoI we recognize that this canonical model may be insufficient. In particular, the causal estimation of x_t defined by the OU model shown in Eq. (2.2), produces estimation errors whose variance is an interval-wise, monotonically growing exponential function of the AoI [9, Sec. II.D].

Although non-linear operations on the AoI, yielding new performance criteria may have also heuristic origins, see [8], we may say that these heuristics are approximations or the implicit attempts to go beyond the simple Markovian Gaussian model from (2.1) and (2.2).

Both the timeliness and the accuracy interpretations of the AoI are (potentially) useful for the design or control of the communication systems. However, the attempts to combine both, e.g., [42, Sec. II.A.2], are not yet based on any formal principle, so here, we rather present an extension of these metrics to the case of non-causal estimation and leave open the issue of their simultaneous usage.

2.2.1 Distortion function

The distortion quantifies the estimation error of the signal reconstructed at the monitor, $\hat{x}_t$ which is affected by the transmission delay. The receiver estimates the measurement signal using the received samples gathered in set

$$\mathscr{X} = \{x_{\tau_1}, x_{\tau_2}, \ldots, x_{\tau_N}\} \tag{2.10}$$

where the sampling instants τ_n are gathered in

$$\mathscr{T} = \{\tau_1, \tau_2, \ldots, \tau_N\}. \tag{2.11}$$

If the signal x_t is Gaussian, the maximum likelihood estimate $\hat{x}_t$ is given by a linear combination of the samples gathered in $\mathscr{X}$ [46, Section 1.4]

$$\hat{x}_t = \mu_t + \sum_{i=1}^{N}\sum_{j=1}^{N} K_{t,\tau_i} K^{-1}_{\tau_i,\tau_j}(x_{\tau_j} - m_{\tau_j}), \tag{2.12}$$

and the distortion function which is defined as the variance of the estimation error is given by

$$\hat{\sigma}_t^2 = \mathbb{E}\left[(\hat{x}_t - x_t)^2\right] = K_{t,t} \sum_{i=1}^{N}\sum_{j=1}^{N} K_{t,\tau_i} K^{-1}_{\tau_i,\tau_j} K_{\tau_j,t}, \tag{2.13}$$

where $\mu_t = \mathbb{E}[x_t]$ and $K_{t_1,t_2} = \mathbb{E}[(x_{t_1} - \mu_{t_1})(x_{t_2} - \mu_{t_2})]$ are the mean and the covariance of the signal x_t.

Since the (Wiener and colored Gaussian noise) models we adopted are Markovian, the estimate $\hat{x}_t$ will depend only on x_{t_-} and x_{t_+}, where

$$t_- = t_-(t) = \max_{\tau \in \mathscr{T}} \{\tau : \tau \le t\}, \tag{2.14}$$

$$t_+ = t_+(t) = \min_{\tau \in \mathscr{T}} \{\tau : \tau \ge t\} \tag{2.15}$$

are the sampling instants closest to t before- and after the time t; their dependence on t will be omitted for sake of clarity. We have now the choice to use the causal estimation, based solely on x_{t_-} or the non-causal one, which may use both x_{t_-} and x_{t_+}. Using (2.12) the causal and non-causal estimations are given by:

$$\hat{x}_t^{\mathrm{c}} = \mu_t + \frac{K_{t,t_-}[x_{t_-} - \mu_{t_-}]}{K_{t_-,t_-}}, \tag{2.16}$$

$$\hat{x}_t^{\mathrm{nc}} = \mu_t + [x_{t_-} - \mu_{t_-}] \frac{K_{t,t_-}K_{t_+,t_+} - K_{t,t_+}K_{t_-,t_+}}{K_{t_-,t_-}K_{t_+,t_+} - K_{t_-,t_+}^2} + [x_{t_+} - \mu_{t_+}] \frac{K_{t,t_+}K_{t_-,t_-} - K_{t_-,t_+}K_{t,t_-}}{K_{t_-,t_-}K_{t_+,t_+} - K_{t_-,t_+}^2}. \tag{2.17}$$

The corresponding estimation error variances for the causal estimation is given by

$$\Delta_t = K_{t,t} - \frac{K_{t,t_-}^2}{K_{t_-,t_-}} \tag{2.18}$$

and for the non-causal estimation, by

$$\delta_t = K_{t,t} - \frac{K_{t,t_-}^2 K_{t_+,t_+} + K_{t,t_+}^2 K_{t_-,t_-}}{K_{t_-,t_-}K_{t_+,t_+} - K_{t_-,t_+}^2} - \frac{2K_{t,t_-}K_{t,t_+}K_{t_-,t_+}}{K_{t_-,t_-}K_{t_+,t_+} - K_{t_-,t_+}^2}. \tag{2.19}$$

These general estimation rules can be now connected to the problem of estimation when the packets must be transmitted from the sensor to the monitor. The fact that the samples are transmitted with a random delay (due to non-perfect transmission channel) affect the formulas.

Let B_m and D_m be respectively the sampling time (generation at the sensor) and the arrival time (at the monitor) of the m-th successfully decoded packet. Moreover, let $\hat{m}(t)$ denote the index of the most recent packet available at time t at the monitor, i.e.,

$$\hat{m}(t) = \mathrm{argmax}_m \{B_m : D_m \leq t\} \tag{2.20}$$

The causal estimation at time t will thus rely on one sample obtained at the time

$$t_{-}^{\mathrm{c}}(t) = B_{\hat{m}(t)}, \tag{2.21}$$

that is, on the most recent packet that already arrived at the monitor.

On the other hand, for the non-causal estimation we will use

$$t_{-}^{\mathrm{nc}}(t) = B_{\check{m}(t)}, \tag{2.22}$$

$$t_{+}^{\mathrm{nc}}(t) = B_{\check{m}(t)+1}; \tag{2.23}$$

where

$$\check{m}(t) = \mathrm{argmax}_m \{B_m : B_m \leq t\} \tag{2.24}$$

is the index of the most recent packet which can be used for the estimation at time t and thus $\check{m}(t)+1$ is the closest future packet. Clearly, the arrival time becomes irrelevant in the calculation. Thus, the causality not only alters the estimation formulas, it also changes the reference samples: compare (2.21) and (2.22) to see that $t_{-}^{\mathrm{c}}(t)$ is not the same as $t_{-}^{\mathrm{nc}}(t)$; for example, from Fig. 2.1, for $t \in (B_2, D_2)$, we have $\hat{m}(t) = 1$ and $\check{m}(t) = 2$, thus $t_{-}^{\mathrm{c}}(t) = B_1$ and $t_{-}^{\mathrm{nc}}(t) = B_2$.

2.2.2 Wiener signal

Using (2.1) we obtain $\mu_t = 0$ and $K_{t_1,t_2} = \min\{t_1, t_2\}$, which applied in (2.16) and (2.17) yield

$$\hat{x}_t^{\mathrm{c}} = x_{t_{-}^{\mathrm{c}}}, \tag{2.25}$$

$$\hat{x}_t^{\mathrm{nc}} = x_{t_{-}^{\mathrm{nc}}} \frac{t_{+}^{\mathrm{nc}} - t}{t_{+}^{\mathrm{nc}} - t_{-}^{\mathrm{nc}}} + x_{t_{+}^{\mathrm{nc}}} \frac{t - t_{-}^{\mathrm{nc}}}{t_{+}^{\mathrm{nc}} - t_{-}^{\mathrm{nc}}}. \tag{2.26}$$

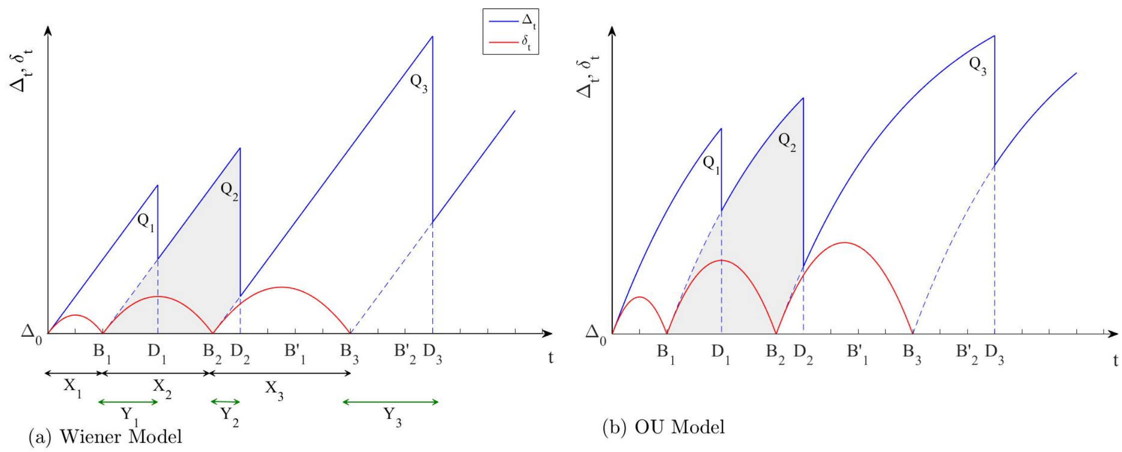

Figure 2.1: Example of the evolution of the distortion function (under the same pattern of packet generation/arrival instants, B_m and D_m), when applying a causal estimation (Δ_t) and non-causal estimation (δ_t), for a) Wiener signal and b) colored Gaussian noise (with $\alpha = 0.1$). The area $Q_2 = Q(X_2, Y_2)$ used in (2.38) is shown in gray.

And the corresponding variances of the distortion function are given by

$$\Delta_t = t - t_-^{\mathrm{c}}, \tag{2.27}$$

$$\delta_t = [t - t_-^{\mathrm{nc}}]\Big[1 - \frac{t - t_-^{\mathrm{nc}}}{t_+^{\mathrm{nc}} - t_-^{\mathrm{nc}}}\Big]. \tag{2.28}$$

We recognize the error variance of causal estimation (2.27) to be the well-known definition of the AoI, [19, Eq. (11)], extensively used in the literature.

We emphasize again that the difference of non-causal distortion with regard to the causal (AoI) is not merely in using additional sample: unlike in the causal, the estimation is not done in real-time; the estimate of the signal $\hat{x}_t$ can be calculated only if the packet m with $B_m > t$ is received at the monitor.

The forms of the causal distortion , Δ_t, and the non-causal distortion, δ_t, are shown in Fig. 2.1, where the piece-wise linear form of the causal distortion is well known, e.g., [25, Fig. 1], while the parabolic shape of δ_t is a consequence of non-causal estimation.

2.2.3 OU Signal

Assuming the steady-state of the model in (2.2), the signal has the mean $\mu_t = 0$ and the covariance:

$$K_{t_1,t_2} = \mathrm{e}^{-\alpha|t_2-t_1|}, \quad \text{where}\alpha = -\log\kappa. \tag{2.29}$$

Following equations (2.18) and (2.19), the estimation results are given by

$$\hat{x}^{\mathrm{c}}_t = \mathrm{e}^{-\alpha(t-t^{\mathrm{c}}_-)} x_{t^{\mathrm{c}}_-} \tag{2.30}$$

$$\hat{x}^{\mathrm{nc}}_t = \frac{x_{t^{\mathrm{nc}}_-}\left[\mathrm{e}^{-\alpha(t-t^{\mathrm{nc}}_-)} - \mathrm{e}^{-\alpha(2t^{\mathrm{nc}}_+-t-t^{\mathrm{nc}}_-)}\right]}{1-\mathrm{e}^{-2\alpha(t^{\mathrm{nc}}_+-t^{\mathrm{nc}}_-)}} + \frac{x_{t^{\mathrm{nc}}_+}\left[\mathrm{e}^{-\alpha(t^{\mathrm{nc}}_+-t)} - \mathrm{e}^{-\alpha(t^{\mathrm{nc}}_++t-2t^{\mathrm{nc}}_-)}\right]}{1-\mathrm{e}^{-2\alpha(t^{\mathrm{nc}}_+-t^{\mathrm{nc}}_-)}}, \tag{2.31}$$

and the variances of the estimation errors by

$$\Delta_t = 1-\mathrm{e}^{-2\alpha(t-t^{\mathrm{c}}_-)}, \tag{2.32}$$

$$\delta_t = 1 - \frac{\mathrm{e}^{-2\alpha(t-t^{\mathrm{nc}}_-)} + \mathrm{e}^{-2\alpha(t^{\mathrm{nc}}_+-t)} - 2\mathrm{e}^{-2\alpha(t^{\mathrm{nc}}_+-t^{\mathrm{nc}}_-)}}{1-\mathrm{e}^{-2\alpha(t^{\mathrm{nc}}_+-t^{\mathrm{nc}}_-)}}. \tag{2.33}$$

We also show the form of Δ_t and δ_t in Fig. 2.1, where we see the non-linear interval-wise monotonic behaviour of Δ_t. This illustrates well that the rationale for using the non-linear function of the age may be sought in the model of the measurement signal.

2.2.4 Model mismatch

In the previous section, we applied the maximum likelihood estimate of the signal where the expression for $\hat{x}_t$ in (2.12) is the optimum linear function resulting into the minimum estimation error in (2.13). Here, with the goal of assessing the impact of the mismatch between assumed and actual model of the signal, we will use the linear interpolation adopted in the Wiener model, i.e., (2.27) and (2.28), to estimate the OU signal as follows:

$$\tilde{x}_t = \sum_{i=1}^{N} \beta_i x_{\tau_i} \tag{2.34}$$

and the subsequent estimation error is then given by [46, Section 1.4]

$$\tilde{L}_t = \mathbb{E}[(x_t - \tilde{x}_t)^2] = K_{t,t} + \sum_{i=1}^{N} \beta_i \sum_{j=1}^{N} K_{\tau_i,\tau_j} \beta_j - 2\sum_{i=1}^{N} \beta_i K_{t,\tau_i}. \tag{2.35}$$

From the linear equations in (2.27) and (2.28), we find immediately β_i and x_{τ_i}, which used in (2.35) yield both, the causal mismatch estimation errors

$$\tilde{\Delta}_t = 2(1 - \mathrm{e}^{-\alpha(t - t_-^{\mathrm{c}})}), \tag{2.36}$$

and the non-causal mismatch estimation error

$$\begin{aligned}\tilde{\delta}(t) = 1 - 2\frac{(t_+ - t)\mathrm{e}^{-\alpha(t-t_-)} + (t - t_-)\mathrm{e}^{-\alpha(t_+ - t)}}{t_+ - t_-} \\ + \frac{(t_+ - t)^2 + (t - t_-)^2 + 2\mathrm{e}^{-\alpha(t_+ - t_-)}(t - t_-)(t_+ - t)}{(t_+ - t_-)^2}.\end{aligned} \tag{2.37}$$

2.2.5 Comparison metrics

In order to compare the transmission strategies and the criteria themselves we have to define the statistical measure of the causal or non-causal distortion functions and here, we opt for their long-term averages defined as

$$\overline{\Delta} = \lim_{T\to\infty} \frac{1}{T} \int_0^T \Delta_t \mathrm{d}t \tag{2.38}$$

$$\overline{\delta} = \lim_{T\to\infty} \frac{1}{T} \int_0^T \delta_t \mathrm{d}t. \tag{2.39}$$

The case of fixed buffer management strategies will be explained in Sec. 2.3 while the adaptive policies will be dealt with in Sec. 2.4.

2.3 Buffer management: fixed policies

To calculate the average causal and non-causal distortion, we take advantage of the fact that both Δ_t and δ_t are renewal processes with random renewal X, i.e., the time between the generation instants of two subsequent packets that were successfully received at the monitor; it has realizations $X_m = B_m - B_{m-1}$. Therefore,

$$\overline{\Delta} = \frac{\mathbb{E}_{X,Y}\left[Q(X,Y)\right]}{\mathbb{E}_X[X]} \tag{2.40}$$

where $Q(X,Y)$ is the shadowed area in Fig. 2.1 and (2.38) is obtained through the renewal-reward theorem [47, Section 2]; Y is the random delivery time, with realization $Y_m = D_m - B_m$.

Similarly we calculate the long-term average non-causal distortion:

$$\overline{\delta} = \frac{\mathbb{E}_X\left[\int_X \delta_t \mathrm{d}t\right]}{\mathbb{E}_X[X]}. \tag{2.41}$$

Quite obviously these metrics depend on the distribution of the random variable X and Y which will change with the sampling strategy, the buffer management policy, or the transmission model. The main difficulty here is to calculate the expected value of the integral in the numerator of (2.38) and (2.39).

Wiener process:

In the case of the Wiener signal at the source and causal estimation, the age (2.27) is a piece-wise linear function of time as also illustrated in Fig. 2.1.

The integral in the numerator of (2.38) may be calculated for an arbitrarily chosen packet m as

$$Q(X_m, Y_m) = \int_{B_{m-1}}^{D_m} (t - B_{m-1})\mathrm{d}t - \int_{B_m}^{D_m} (t - B_m)\mathrm{d}t = \frac{1}{2}(X_m + Y_m)^2 - \frac{1}{2}Y_m^2. \tag{2.42}$$

Applying expectation to (2.42) and from independence of X_m and Y_m, we obtain the well known formula for the average AoI (2.40) [29, Sec. 3-4, (3-25)]

$$\overline{\Delta} = \frac{\mathbb{E}_X[X^2]}{2\,\mathbb{E}_X[X]} + \mathbb{E}_Y[Y]. \tag{2.43}$$

Similar calculation for the non-causal distortion requires calculation of the integral in (2.39)

$$\int_{B_{m-1}}^{B_m} \delta_t \mathrm{d}t = \int_{B_{m-1}}^{B_m} (t - B_{m-1})\left(1 - \frac{t - B_{m-1}}{X_m}\right)\mathrm{d}t = \frac{1}{6}X_m^2 \tag{2.44}$$

which yields the average non-causal distortion

$$\overline{\delta} = \frac{\mathbb{E}_X[X^2]}{6\,\mathbb{E}_X[X]}. \tag{2.45}$$

OU process:

Repeating the above analysis we calculate the integral for Δ_t (2.32)

$$\begin{aligned} Q(X_m, Y_m) &= X_m + \int_{B_m}^{D_m} \mathrm{e}^{-2\alpha(t-B_m)}\mathrm{d}t - \int_{B_{m-1}}^{D_m} \mathrm{e}^{-2\alpha(t-B_{m-1})}\mathrm{d}t \\ &= X_m + \frac{1}{2\alpha}(\mathrm{e}^{-2\alpha(X_m+Y_m)} - \mathrm{e}^{-2\alpha Y_m}), \end{aligned} \tag{2.46}$$

which, after straightforward algebra, and using (2.38) yields

$$\overline{\Delta} = 1 + \frac{\mathbb{E}[\mathrm{e}^{-2\alpha(X+Y)}] - \mathbb{E}[\mathrm{e}^{-2\alpha Y}]}{2\alpha\,\mathbb{E}[X]}. \tag{2.47}$$

A similar calculation for non-causal distortion related to the OU process yields

$$\begin{aligned} \int_{B_{m-1}}^{B_m} \delta_t \mathrm{d}t =& X_m + \frac{2X_m \mathrm{e}^{-2\alpha X_m}}{1-\mathrm{e}^{-2\alpha X_m}} - \frac{\int_{B_{m-1}}^{B_m} \mathrm{e}^{-2\alpha(t-B_{m-1})}\mathrm{d}t}{1-\mathrm{e}^{-2\alpha X_m}} - \frac{\int_{B_{m-1}}^{B_m} \mathrm{e}^{-2\alpha(B_m-t)}\mathrm{d}t}{1-\mathrm{e}^{-2\alpha X_m}} \\ =& X_m + \frac{2X_m \mathrm{e}^{-2\alpha X_m}}{1-\mathrm{e}^{-2\alpha X_m}} - \frac{1}{\alpha}, \end{aligned} \tag{2.48}$$

from which the average non-causal distortion is obtained

$$\overline{\delta} = 1 - \frac{1}{\alpha\,\mathbb{E}[X]} + \frac{2\,\mathbb{E}[\frac{X\mathrm{e}^{-2\alpha X}}{1-\mathrm{e}^{-2\alpha X}}]}{\mathbb{E}[X]}. \tag{2.49}$$

Model mismatch:

Following the same integration as in (2.46) and (2.48), we can calculate the long term average of the mismatched causal and non-causal distortion, respectively:

$$\overline{\tilde{\Delta}} = 2\left(1 + \frac{\mathbb{E}[\mathrm{e}^{-\alpha(X+Y)}] - \mathbb{E}[\mathrm{e}^{-\alpha Y}]}{\alpha\,\mathbb{E}[X]}\right) \tag{2.50}$$

$$\bar{\tilde{\delta}} = \frac{5}{3} + \frac{\mathbb{E}[X\mathrm{e}^{-\alpha X}]}{3\,\mathbb{E}[X]} + \frac{4\,\mathbb{E}[\frac{1}{X}]}{\alpha^2\,\mathbb{E}[X]} - \frac{4\,\mathbb{E}[\frac{\mathrm{e}^{-\alpha X}}{X}]}{\alpha^2\,\mathbb{E}[X]} - \frac{4}{\alpha\,\mathbb{E}[X]}. \tag{2.51}$$

Now, to calculate the average causal and non-causal distortion for the particular model and chosen estimation (optimal Wiener and OU estimation, or the mismatched model estimation) we have to calculate the moments of X and the expectation of exponential functions of X which are required in (2.43), (2.45), (2.47), (2.49), (2.50), and (2.51).

The focus of the following sections is to find the expectations analytically. We note, however, that even if it cannot be done, these quantities depend only on the sampling strategy and transmission method so they may be obtained by simulations which are much more straightforward to carry out that those necessary to implement (2.38) or (2.39).

2.3.1 Preemption Policy

Under this policy, a packet in service is removed from the buffer if a new packet is generated at the sensor. Thus, we decompose the inter-renewal time, X, into three consecutive terms

$$X = I + F + Y, \tag{2.52}$$

where I is the waiting time to receive a new sample in the sensor buffer once a packet under service is decoded successfully in the monitor. F is the time when the server is busy with transmission of preempted packets in between two consecutive successfully decoded ones.

First, we calculate the distribution of I. Since the packet arrival process is geometric and hence memoryless, the waiting time will be geometric with the parameter λ and the following probability generating function

$$G_I(z) = \mathbb{E}[\mathrm{e}^{zI}] = \frac{\lambda}{1-(1-\lambda)z}. \tag{2.53}$$

Calculating the second term of the inter-renewal, F, we need to quantify the time duration spent serving the preempted packets in-between two consecutive successfully decoded packets.

Proposition 2.3.1. *The probability generating function of F under ARQ and HARQ is given by:*

$$G_F(z) = \begin{cases} \frac{(1-\varepsilon)(1-z(1-\lambda)\varepsilon)}{(1-\varepsilon(1-\lambda))(1-z\varepsilon)} & \textit{ARQ} \\ \frac{\mathrm{e}^{-\theta\lambda}(1-(1-\lambda)z)}{1-z(1-\lambda\mathrm{e}^{-\theta(1-(1-\lambda)z)})} & \textit{HARQ} \end{cases} \tag{2.54}$$

Proof. See Appendix A. □

To find the expectation of Y (needed in (2.43)), we start with the distribution $\Pr\{Y=k\} = \Pr\{S=k|R\geq k\}$,

$$Y \sim \begin{cases} \text{Geom}\big(1-\varepsilon(1-\lambda)\big) & \text{ARQ} \\ \text{Pois}\big(\theta(1-\lambda)\big) & \text{HARQ} \end{cases} \tag{2.55}$$

and then, obtaining the PGF and moment as

$$G_Y(z) = \begin{cases} \frac{z(1-\varepsilon(1-\lambda))}{1-z\varepsilon(1-\lambda)} & \text{ARQ} \\ z\mathrm{e}^{-\theta(1-\lambda)(1-z)} & \text{HARQ} \end{cases} \tag{2.56}$$

$$\mathbb{E}[Y] = \begin{cases} \frac{1}{1-\varepsilon(1-\lambda)} & \text{ARQ} \\ 1+\theta(1-\lambda) & \text{HARQ} \end{cases} \tag{2.57}$$

and replacing z by $\mathrm{e}^{-2\alpha Y}$ in (2.56)

$$\mathbb{E}[\mathrm{e}^{-2\alpha Y}] = \begin{cases} \frac{\mathrm{e}^{-2\alpha}(1-\varepsilon(1-\lambda))}{1-\mathrm{e}^{-2\alpha}\varepsilon(1-\lambda)} & \text{ARQ} \\ \mathrm{e}^{-\theta(1-\lambda)(1-\mathrm{e}^{-2\alpha})-2\alpha} & \text{HARQ} \end{cases}. \tag{2.58}$$

From the independence of the random variables$I$, F and Y in (2.52), the PGF of X will be

$$G_X(z) = G_I(z)G_F(z)G_Y(z) = \begin{cases} \frac{(z(1-\varepsilon)\lambda)}{(1-z\varepsilon)(1-z(1-\lambda))} & \text{ARQ} \\ \frac{\lambda z\mathrm{e}^{-\theta(1-(1-\lambda)z)}}{1-z(1-\lambda\mathrm{e}^{-\theta(1-(1-\lambda)z)})} & \text{HARQ} \end{cases} \tag{2.59}$$

and the n-th moment of X can be obtained by placing $z=1$ in the n-th derivative of $G_X(z)$. Consequently, the first and second moments of X are

$$\mathbb{E}[X] = \begin{cases} \frac{1-\varepsilon(1-\lambda)}{\lambda(1-\varepsilon)} & \text{ARQ} \\ \frac{1}{p\lambda} & \text{HARQ} \end{cases} \tag{2.60}$$

$$\mathbb{E}[X^2] = \begin{cases} \frac{2\varepsilon\lambda^2+(1-\varepsilon(1-\lambda))(2-\lambda)(1-\varepsilon)}{(1-\varepsilon)^2\lambda^2} & \text{ARQ} \\ \frac{2-p\lambda-2p\theta\lambda(1-\lambda)}{\lambda^2 p^2} & \text{HARQ} \end{cases} \tag{2.61}$$

p is obtained from (A.1) in Appendix A. Then, the expectation of function $\mathrm{e}^{-2\alpha X}$ will be

$$\mathbb{E}[\mathrm{e}^{-2\alpha X}] = \mathbb{E}[\mathrm{e}^{-2\alpha I}]\,\mathbb{E}[\mathrm{e}^{-2\alpha B}]\,\mathbb{E}[\mathrm{e}^{-2\alpha Y}] = \begin{cases} \frac{(\mathrm{e}^{-2\alpha}(1-\varepsilon)\lambda)}{(1-\mathrm{e}^{-2\alpha}\varepsilon)(1-\mathrm{e}^{-2\alpha}(1-\lambda))} & \text{ARQ} \\ \frac{\lambda\mathrm{e}^{-\theta(1-(1-\lambda)\mathrm{e}^{-2\alpha})-2\alpha}}{1-\mathrm{e}^{-2\alpha}(1-\lambda\mathrm{e}^{-\theta(1-(1-\lambda)\mathrm{e}^{-2\alpha})})} & \text{HARQ} \end{cases} \tag{2.62}$$

Finally, using (2.60), (2.61) and (2.57) in (2.43) yields the average causal distortion:

$$\overline{\Delta}_{\text{Wiener}}^{\text{preemption}} = \begin{cases} \frac{2(1-\varepsilon)+\lambda(1+\varepsilon)}{2\lambda(1-\varepsilon)} & \text{ARQ} \\ \frac{\lambda+2\mathrm{e}^{\theta\lambda}}{2\lambda} & \text{HARQ} \end{cases} \tag{2.63}$$

$$\overline{\Delta}_{\text{OU}}^{\text{preemption}} = \begin{cases} 1-\frac{\lambda(1-\varepsilon)\mathrm{e}^{-2\alpha}(1-\mathrm{e}^{-2\alpha})}{2\alpha(1-\varepsilon\mathrm{e}^{-2\alpha})(1-(1-\lambda)\mathrm{e}^{-2\alpha})} & \text{ARQ} \\ 1-\frac{\lambda\mathrm{e}^{-\theta(1-Q)-2\alpha}(1-\mathrm{e}^{-2\alpha})}{2\alpha(1-(1-\lambda\mathrm{e}^{-\theta(1-Q)})\mathrm{e}^{-2\alpha})} & \text{HARQ} \end{cases}, \tag{2.64}$$

where $Q=(1-\lambda)\mathrm{e}^{-2\alpha}$.

The expectation of $\frac{X\mathrm{e}^{-2\alpha X}}{1-\mathrm{e}^{-2\alpha X}}$ may be calculated from

$$\mathbb{E}[\frac{X\mathrm{e}^{-2\alpha X}}{1-\mathrm{e}^{-2\alpha X}}] = \mathbb{E}[X\sum_{n=1}^{\infty}\mathrm{e}^{-2\alpha Xn}] = \sum_{n=1}^{\infty}\mathbb{E}[X\mathrm{e}^{-2n\alpha X}] \tag{2.65}$$

where the expectation of function $X\mathrm{e}^{-2n\alpha X}$ is given in the following.

Proposition 2.3.2.

$$\mathbb{E}[X\mathrm{e}^{-2n\alpha X}] = \begin{cases} \frac{\lambda(1-\varepsilon)\mathrm{e}^{-2n\alpha}(1-\varepsilon(1-\lambda)\mathrm{e}^{-4n\alpha})}{(1-(1-\lambda)\mathrm{e}^{-2n\alpha})^2(1-\varepsilon\mathrm{e}^{-2n\alpha})^2} & \text{ARQ} \\ \frac{\lambda Q_n \mathrm{e}^{-\theta(1+\lambda)}U}{(1-\lambda)(1-Q_n)} & \text{HARQ} \end{cases} \tag{2.66}$$

in which U and Q_n are given by (B.7) *and* (B.5) *in Appendix B.*

Proof. See Appendix B. □

The average non-causal distortion is given by

$$\overline{\delta}^{\text{preemption}}_{\text{Wiener}} = \begin{cases} \frac{(3-\varepsilon-(1-\lambda)(1+\varepsilon))(1-\varepsilon(1-\lambda))-2\lambda(1-\varepsilon)}{6\lambda(1-\varepsilon)(1-\varepsilon(1-\lambda))} & \text{ARQ} \\ \frac{2-\lambda\mathrm{e}^{-\theta\lambda}(1+2\theta(1-\lambda))}{6\lambda\mathrm{e}^{-\theta\lambda}} & \text{HARQ} \end{cases} \tag{2.67}$$

and by

$$\overline{\delta}^{\text{preemption}}_{\text{OU}} = \begin{cases} 1-\frac{\lambda(1-\varepsilon)(1-2\alpha\sum_{n=1}^{\infty}\mathbb{E}[X\mathrm{e}^{-2n\alpha X}])}{\alpha(1-\varepsilon(1-\lambda))} & \text{ARQ} \\ 1-\frac{\lambda\mathrm{e}^{-\theta\lambda}(1-2\alpha\sum_{n=1}^{\infty}\mathbb{E}[X\mathrm{e}^{-2n\alpha X}])}{\alpha} & \text{HARQ} \end{cases} \tag{2.68}$$

2.3.2 Blocking Policy

The blocking policy ignores any new arrival when there is an ongoing transmission in the system. Because of the memoryless property of the interarrival process, we thus have

$$X = S + I, \tag{2.69}$$

where S follows the definition in (2.8) and I is defined by (2.53). Following the same procedure as in the previous section, the PGF of X may be derived as

$$G_X(z) = \begin{cases} \frac{z\lambda(1-\varepsilon)}{(1-z\varepsilon)(1-z(1-\lambda))} & \text{ARQ} \\ \frac{z\mathrm{e}^{-\theta(1-z)}\lambda}{1-(1-\lambda)z} & \text{HARQ} \end{cases}, \tag{2.70}$$

from which we obtain the following:

$$\mathbb{E}[X] = \begin{cases} \frac{1-\varepsilon(1-\lambda)}{\lambda(1-\varepsilon)} & \text{ARQ} \\ \frac{1+\theta\lambda}{\lambda} & \text{HARQ} \end{cases} \tag{2.71}$$

$$\mathbb{E}[X^2] = \begin{cases} \frac{2\varepsilon\lambda^2+(1-\varepsilon(1-\lambda))(2-\lambda)(1-\varepsilon)}{(1-\varepsilon)^2\lambda^2} & \text{ARQ} \\ \theta(3+\theta)+\frac{1+(1-\lambda)(1+2\theta\lambda)}{\lambda^2} & \text{HARQ} \end{cases} \tag{2.72}$$

$$\mathbb{E}[\mathrm{e}^{-2\alpha X}] = \begin{cases} \frac{\lambda(1-\varepsilon)\mathrm{e}^{-2\alpha}}{(1-\mathrm{e}^{-2\alpha}\varepsilon)(1-\mathrm{e}^{-2\alpha}(1-\lambda))} & \text{ARQ} \\ \mathrm{e}^{-2\alpha-\theta(1-\mathrm{e}^{-2\alpha})}\frac{\lambda}{1-(1-\lambda)\mathrm{e}^{-2\alpha}} & \text{HARQ} \end{cases} \tag{2.73}$$

Thus, using (2.71) and (2.72) in (2.43) and (2.32), we obtain the following:

$$\overline{\Delta}_{\text{Wiener}}^{\text{blocking}} = \begin{cases} \frac{(1-\varepsilon)^2(1-\lambda)(2-\lambda)-\lambda^2(1-3\varepsilon)+2\lambda(2-2\varepsilon+\varepsilon\lambda)}{2\lambda(1-\varepsilon)(1-\varepsilon(1-\lambda))} & \text{ARQ} \\ \frac{\lambda(1+\theta)(2+3\theta\lambda)-\lambda(1-2\theta)+2}{2\lambda(1+\theta\lambda)} & \text{HARQ} \end{cases} \tag{2.74}$$

$$\overline{\Delta}_{\text{OU}}^{\text{blocking}} = \begin{cases} 1-\frac{\lambda(1-\varepsilon)^2\mathrm{e}^{-2\alpha}(1-\mathrm{e}^{-2\alpha})(1-\varepsilon(1-\lambda)\mathrm{e}^{-2\alpha})}{2\alpha(1-\varepsilon\mathrm{e}^{-2\alpha})^2(1-\varepsilon(1-\lambda))(1-(1-\lambda)\mathrm{e}^{-2\alpha})} & \text{ARQ} \\ 1-\frac{\lambda\mathrm{e}^{-\theta(1-\mathrm{e}^{-2\alpha})-2\alpha}(1-\mathrm{e}^{-2\alpha}(1-\lambda(1-\mathrm{e}^{-\theta(1-\mathrm{e}^{-2\alpha})})))}{2\alpha(1+\theta\lambda)(1-(1-\lambda)\mathrm{e}^{-2\alpha})} & \text{HARQ} \end{cases} \tag{2.75}$$

$\mathbb{E}[\frac{X\mathrm{e}^{-2\alpha X}}{1-\mathrm{e}^{-2\alpha X}}]$ is calculated as in (2.65) and to compute $\mathbb{E}[X\mathrm{e}^{-2n\alpha X}]$ we use the following:

Proposition 2.3.3.

$$\mathbb{E}[X\mathrm{e}^{-2n\alpha X}] = \begin{cases} \frac{\lambda(1-\varepsilon)\mathrm{e}^{-2n\alpha}(1-\varepsilon(1-\lambda)\mathrm{e}^{-4n\alpha})}{(1-(1-\lambda)\mathrm{e}^{-2n\alpha})^2(1-\varepsilon\mathrm{e}^{-2n\alpha})^2} & \text{ARQ} \\ \frac{\lambda\mathrm{e}^{-\theta(1-\mathrm{e}^{-2n\alpha})-2n\alpha}(1+(1-Q_n)\theta\mathrm{e}^{-2n\alpha})}{(1-(1-\lambda)\mathrm{e}^{-2n\alpha})^2} & \text{HARQ} \end{cases} \tag{2.76}$$

where Q_n is provided in (B.5) *in Appendix B.*

Proof. See Appendix C. □

The non-causal distortion is calculated for the Wiener process as

$$\overline{\delta}_{\text{wiener}}^{\text{blocking}} = \begin{cases} \frac{(3-\varepsilon-(1-\lambda)(1+\varepsilon))(1-\varepsilon(1-\lambda))-2\lambda(1-\varepsilon)}{6\lambda(1-\varepsilon)(1-\varepsilon(1-\lambda))} & \text{ARQ} \\ \frac{\lambda(1+\theta)(2+3\theta\lambda)-\lambda(1-2\theta)+2-2\lambda(1+\theta)(1+\theta\lambda)}{6\lambda(1+\theta\lambda)} & \text{HARQ} \end{cases}, \tag{2.77}$$

and for the OU process as

$$\overline{\delta}_{\text{OU}}^{\text{blocking}} = \begin{cases} 1-\frac{\lambda(1-\varepsilon)(1-2\alpha\sum_{n=1}^{\infty}\mathbb{E}[X\mathrm{e}^{-2n\alpha X}])}{\alpha(1-\varepsilon(1-\lambda))} & \text{ARQ} \\ 1-\frac{\lambda(1-2\alpha\sum_{n=1}^{\infty}\mathbb{E}[X\mathrm{e}^{-2n\alpha X}])}{\alpha(1+\theta\lambda)} & \text{HARQ} \end{cases}. \tag{2.78}$$

2.4 Buffer management: optimal controller

Instead of fixing the buffer management policy to block or to preempt, we may decide which action should be taken at each given time slot t. This is the problem of finding the optimal decision and recognizing the Markovian nature of the process, the problem of finding the optimal actions will be formulated here using the framework of the MDP.

Our objective will be defined as the minimization of the average (causal or non-causal) estimation errors and it has to be formulated via the cost function attributed to a particular transition from the *state* at time t to the state at time $t+1$.

2.4.1 MDP Formulation

The infinite-horizon MDP problem can be described by the following elements:

- The state space $\mathscr{S}$, where the state at time t is defined by the tuple $s_t = (\Delta_t, d_t, r_t)$, where Δ_t is the causal distortion at the beginning of the time slot t, i.e., time since the generation of a last successfully delivered packet as defined in (2.27).

  The time elapsed since the generation of the packet currently under service is denoted by d_t; if there is no packet in the buffer we set $d_t = 0$.

  The generation of a new packet at the sensor is indicated by $r_t = 1$, otherwise $r_t = 0$.

- The action, a_t, depends on the state, i.e., $a_t = \pi[s_t]$ with $\pi[\cdot]$ being the policy. We use $a_t = 0$

$$P_a(s,s') = \begin{cases} \Pr(r')g(d) & \text{if } a=0, \Delta'=\Delta+1, d'=d+1,\ \forall r; \\ \Pr(r')(1-g(d)) & \text{if } a=0, \Delta'=d+1, d'=0,\ \forall r; \\ \Pr(r')g(0) & \text{if } a=1, \Delta'=\Delta+1, d'=1,\ r=1; \\ \Pr(r')(1-g(0)) & \text{if } a=1, \Delta'=1, d'=0,\ r=1; \\ \Pr(r') & \text{if } a=0, \Delta'=\Delta+1, d'=0,\ r=0; \\ \Pr(r') & \text{if } \Delta'=1, \Delta=\Delta_{\max}, d'=0; \\ 0 & \text{otherwise.} \end{cases} \tag{2.80}$$

to denote the blocking of the newly generated packet, and $a_t = 1$ denotes preemption.

Now, we have to determine the policy $\pi[\cdot]$ for all states when the packet is under service and a new packet is generated at the sensor (i.e., when $r_t = 1$ and $d_t > 0$). The actions are predefined as i) $\pi[(\Delta,0,1)] = 1$, i.e., always accept the new packet when the buffer is empty, ii) $\pi[(\Delta,d,0)] = 0$, i.e., continue transmission in the absence of a new packet.

- The state-transition probability $P_a(s,s') = \Pr\{s_{t+1} = s' | s_t = s, a_t = a\}$ is shown in (2.80) where we take into account two independent random events: the packet generation at the sensor and the transmission error. The conditional probability of the latter is obtained from (2.7) (shown in (2.79)) and depends on the round number d when HARQ is used, while for ARQ the retransmission errors are independent, see (2.8).

$$g(d) = \Pr\{\text{NACK}_d | \text{NACK}_{d-1}\} = \begin{cases} \varepsilon & \text{ARQ} \\ \frac{\gamma(\theta,d+1)}{\gamma(\theta,d)} & \text{HARQ} \end{cases}, \tag{2.79}$$

- The function $C(s,s')$ is the *cost* associated with the transition from the state s (at time t) to the state s' (at time $t+1$); in our case, the transition cost is independent from the action $a_t = \pi[s_t]$.

  In both causal and non-causal estimations we adopt the perspective similar to the one we already used when analyzing the fixed policies in Sec. 2.3: the non-zero cost is incurred only at the renewal, i.e., after the ACK message is received

$$C(s,s') = q(s,s')J(s,s') \tag{2.81}$$

where $q(s,s') = (\mathbb{1}_{d>0} + \mathbb{1}_{d=0}\mathbb{1}_{r=1})\mathbb{1}_{d'=0}$ is the indicator of the decoding feedback received at the beginning of the state s' (informing the sensor at time $t+1$ that the packet sent at time slot t was correctly received); $\mathbb{1}_z = 1$ if z is true, and $\mathbb{1}_z = 0$ otherwise.

As for the cost value $J(s,s')$, we identify the service time as $Y_{\check{m}} = \Delta'$ and $X_{\check{m}} + Y_{\check{m}} = \Delta + 1$; here $\check{m}$ denotes the index of the packet as defined in (2.24). So reusing (2.42) and (2.46) in case of the causal estimation we obtain

$$J(s,s') = \begin{cases} \frac{1}{2}((\Delta+1)^2 - \Delta'^2) & \text{Wiener} \\ X' + \frac{1}{2\alpha}(\mathrm{e}^{-2\alpha(\Delta+1)} - \mathrm{e}^{-2\alpha\Delta'}) & \text{OU} \end{cases}, \tag{2.82}$$

while, using (2.44) and (2.48) in case of non-causal estimation yields

$$J(s,s') = \begin{cases} \frac{X_{\check{m}}^2}{6} & \text{Wiener} \\ X_{\check{m}} + \frac{2\mathrm{e}^{-2\alpha X_{\check{m}}}}{1-\mathrm{e}^{-2\alpha X_{\check{m}}}} - \frac{1}{\alpha} & \text{OU} \end{cases}. \tag{2.83}$$

We emphasize that the cost (2.82) and (2.83) need to be calculated only at the packet arrival, i.e., when $q(s,s') = 1$.

Given an observed system state $s_t \in \mathscr{S}$ the transmitter (at the sensor) must determine the buffer management action $a_t = \pi[s_t]$; i.e., it has to find a state-dependent policy $\pi[\cdot]$.

The long-term average variance of the estimation error in the monitor is given by

$$V_\pi = \lim_{T\to+\infty} \frac{1}{T+1} \sum_{t=0}^{T} C(s_t, s_{t+1}), \tag{2.84}$$

which depends on the policy $\pi[\cdot]$ via the state-transition probability $P_{\pi[s_t]}(s_t, s_{t+1})$.

2.4.2 MDP Optimal Policies

Considering the problem and the designed MDP formulation, we can anticipate the optimal policies as stated in the following.

Proposition 2.4.1. *In ARQ scheme and causal estimation, the optimal policy is $\pi[s_t] = 1$. That is, to minimize $\overline{\Delta}$, the preemption should be always use with Wiener and OU signals.*

Proof. See Appendix D. $\square$

From Propositions 2.4.1, we do no need do analyze the policy for ARQ in case of causal estimation. To optimize (2.84) in all other scenarios the following value iteration is adjusted

$$v^{k+1}(s) = \min_{a \in \{0,1\}} \sum_{s'} P_a(s,s')[C(s,s') + \eta v^k(s')] \tag{2.85}$$

which, starting from an initial $v^0(s)$ $\forall s$ with a discount factor η (we used $\eta = 0.98$), iterates over k till $\forall s, |v^{k+1}(s) - v^k(s)| < \omega$ (we used $\omega = 10^{-4}$); the optimal action for the state s is the argument a which minimizes the right-hand-side of (2.85).

The value iteration can be applied only on the finite state space $\mathscr{S}$ and this condition does not materialize because there is no intrinsic limit on the values of Δ_t and d_t in our problem. Thus, the solution can be obtained only approximately by truncating the state space to $\overline{\mathscr{S}} = \{s \in \mathscr{S} : \Delta \leq \Delta_{\max}, d < \Delta_{\max}\}$; since $d \leq \Delta$ the truncation of d is not restrictive.

Since there cannot be any absorbing state, once $\Delta = \Delta_{\max}$ we force the transition to state $s' = (1,0,r)$; this is shown in (2.80). We also assume that this transition was provoked by the ACK message ant thus we set $q(s,s') = 1$ so the results we obtain is an upper bound on the average cost V_π but the effect of truncation is negligible for large $\Delta_{\max} = 50$ that we used here.

2.5 Numerical Results

Given that the delivery time depends on the transmission errors, non-trivial results are obtained in low SNR, or equivalently at high error channel. For high SNR, most of the packets are delivered in one time slot so ARQ and HARQ are de facto equivalent, and the buffer management blocking/preemption policies do not affect the results. The value of low SNR is $\mathsf{snr} = -3$dB (in which case $\varepsilon = 0.7$) and high SNR is $\mathsf{snr} = +3$dB ($\varepsilon = 0.3$). The examples shown here will be based on the analytical formulas (lines), which will be shown together with the Monte-Carlo simulation (markers).

2.5.1 Wiener Signal

Causal Estimation

With the equations at hand, we can compare preemption and blocking strategies under ARQ and HARQ protocols, whose results are distinguished via sub-indices $(\cdot)_{\text{ARQ}}$ and $(\cdot)_{\text{HARQ}}$. We make the following observations

- For any $\lambda < 1$

$$\lim_{\varepsilon \to 1} \frac{\overline{\Delta}_{\text{ARQ}}^{\text{preemption}}}{\overline{\Delta}_{\text{HARQ}}^{\text{preemption}}} = \infty, \tag{2.86}$$

  that is, in low SNR, the preemption exploits the benefit of HARQ.

- For $\lambda \approx 1$, we quantify the advantage of preemption over blocking in low SNR for ARQ

$$\frac{\overline{\Delta}_{\text{ARQ}}^{\text{blocking}}}{\overline{\Delta}_{\text{ARQ}}^{\text{preemption}}} \approx \frac{3+\varepsilon}{3-\varepsilon} > 1. \tag{2.87}$$

  We note that the same qualitative conclusion was drawn in [25]. Although this can be concluded directly from Proposition 2.4.1, the advantage is that we can quantify the gain and see it is bound by 2 (when $\varepsilon = 1$).

- Observe that $\overline{\Delta}$ is monotonically decreasing with λ in all cases but for HARQ with preemption, where by deriving (2.63) with respect to λ we find the minimum of $\Delta_{\text{HARQ}}^{\text{preemption}}$ for $\hat{\lambda} = \min\{\frac{1}{\theta}, 1\}$. Thus, there may exist a non-trivial $\hat{\lambda} < 1$ which minimizes $\overline{\Delta}$ if preemption is used, e.g., $\hat{\lambda} \approx 0.7$ in Fig. 2.2.

- The case of HARQ is described by

$$\frac{\overline{\Delta}_{\text{HARQ}}^{\text{blocking}}}{\overline{\Delta}_{\text{HARQ}}^{\text{preemption}}} = \frac{(1+3\theta\lambda)[1+\lambda(1+\theta)]+1}{(1+\theta\lambda)(\lambda+2\mathrm{e}^{\theta\lambda})} \tag{2.88}$$

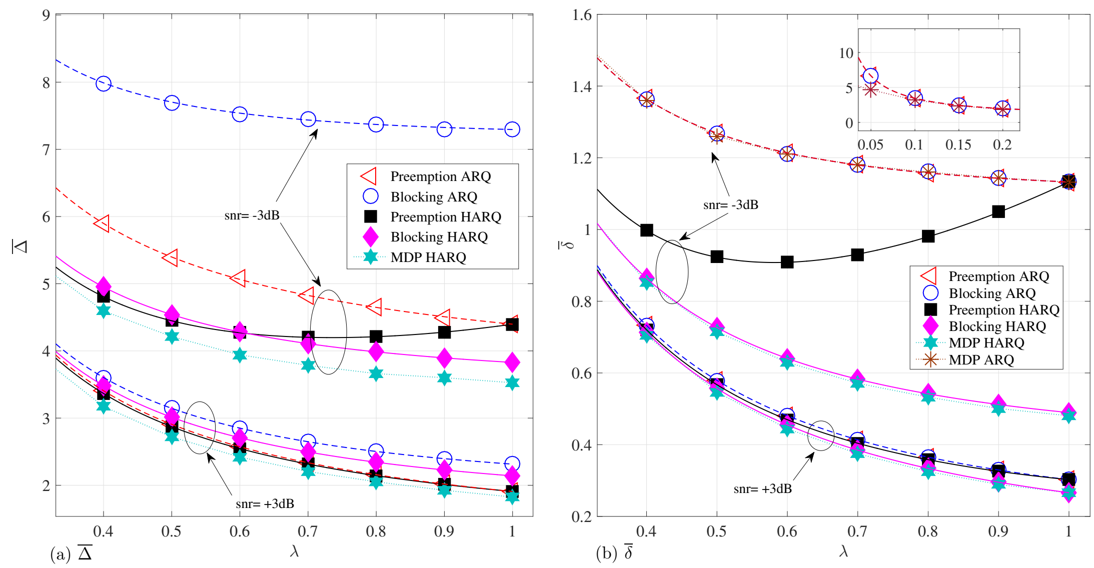

Figure 2.2: a) $\overline{\Delta}$ vs λ and b) $\overline{\delta}$ vs λ, for Wiener process with $\mathsf{snr} = -3$dB and $\mathsf{snr} = +3$dB; Monte-Carlo simulations (markers) and analytical results (lines).

and, noting that the denominator grows with θ exponentially and the denominator – quadratically, we find that

$$\forall\lambda \quad \exists \hat{\mathsf{snr}}, \quad \mathsf{snr} < \hat{\mathsf{snr}} \iff \frac{\overline{\Delta}^{\text{blocking}}_{\text{HARQ}}}{\overline{\Delta}^{\text{preemption}}_{\text{HARQ}}} < 1. \tag{2.89}$$

Thus, the advantage of blocking/preemption depends on the SNR being below/above a threshold $\hat{\mathsf{snr}}$: see Fig. 2.2 for case of low SNR ($\mathsf{snr} < \hat{\mathsf{snr}}$) and high SNR ($\mathsf{snr} > \hat{\mathsf{snr}}$); $\hat{\mathsf{snr}}$ must be found numerically equating (2.88) to one; e.g., for $\lambda = 1$, $\hat{\mathsf{snr}} = -1.5$dB. Here, unlike [12] where blocking was preferred over preemption, we are able to identify the condition (in terms of the SNR) under which one buffer management strategy outperforms the other.

Non-Causal Estimation

By analysing the derived equations, we can conclude that:

- From (2.67) and (2.77), we observe $\overline{\delta}^{\text{blocking}}_{\text{ARQ}} = \overline{\delta}^{\text{preemption}}_{\text{ARQ}}$.

- By comparing (2.67) and (2.77) we find that

$$\frac{\overline{\delta}_{\text{HARQ}}^{\text{blocking}}}{\overline{\delta}_{\text{HARQ}}^{\text{preemption}}} < 1 \quad \forall \mathsf{snr}, \lambda \tag{2.90}$$

which indicates that using HARQ, the (fixed) blocking policy should be always preferred to the (fixed) preemption; this is clear in Fig. 2.2.

- By deriving (2.78) with respect to λ, $\overline{\delta}_{\text{HARQ}}^{\text{blocking}}$ is shown to decrease monotonically with λ. Now, by deriving (2.67) we find that the minimum of $\overline{\delta}_{\text{HARQ}}^{\text{preemption}}$ is obtained for $\hat{\lambda} \leq 1$: e.g., $\hat{\lambda} \approx 0.5$ for $\overline{\mathsf{snr}} = -3\text{dB}$, see Fig. 2.2. As the SNR increases ($\mathsf{snr} = +3\text{dB}$), we have $\hat{\lambda} = 1$.

- Comparing (2.43) and (2.45) we note that

$$\overline{\Delta} = 3\overline{\delta} + \mathbb{E}[Y] \tag{2.91}$$

and, since $\mathbb{E}[Y]$ is always larger in blocking (then we have $Y = S$, so we can compare (2.9) with (2.57)), the average causal distortion, $\overline{\Delta}$ is affected by blocking. This may be seen in Fig. 2.2 for $\mathsf{snr} = 3\text{dB}$: even if $\overline{\delta}_{\text{HARQ}}^{\text{blocking}} < \overline{\delta}_{\text{HARQ}}^{\text{preemption}}$, we have $\overline{\Delta}_{\text{HARQ}}^{\text{blocking}} > \overline{\Delta}_{\text{HARQ}}^{\text{preemption}}$.

On the other hand, with sufficiently low value of $\overline{\delta}_{\text{HARQ}}^{\text{blocking}}$, the advantage of blocking over preemption may be preserved even in causal estimation. This can be observed in Fig. 2.2 for $\mathsf{snr} = -3\text{dB}$.

Optimal policies

The results based on optimal policies obtained by solving the MDP are also shown in Fig. 2.2.

Under the optimal policy $\pi[\cdot]$, the average $\overline{\Delta}$ and $\overline{\delta}$ decrease with respect to the fixed policies, hence, $\pi[\cdot]$ must consist of a mixture of preemption and blocking which, indeed, we found it by inspecting $\pi[\cdot]$.

Nevertheless, in non-causal estimation, the overall tendency in HARQ is towards blocking. The reason for this behaviour is intuitively clear: under blocking, HARQ increases significantly the probability of successful packet decoding (i.e., shortens X) which, quadraticaly decreases the variance of the error. Mathematically, this can be seen comparing $\mathbb{E}[X]$ under preemption, (2.60), and blocking, (2.71), where the latter is smaller.

2.5.2 OU Signal: the optimal and mismatch models

When analyzing the colored Gaussian noise (OU), the most obvious observation is that, having the unitary variance, the estimation error is always bounded applying any linear function for reconstruction. When using the maximum likelihood estimation, the boundary is

$$\overline{\Delta}, \overline{\delta} \leq 1, \tag{2.92}$$

which is different from the estimation error for the Wiener signal which can be unbounded.

Causal and Non-causal Estimation

We do not show here the results for the ARQ because they are qualitatively similar as in those obtained for the Wiener signal (blocking is inferior to preemption):

$$\frac{\overline{\Delta}_{\text{ARQ}}^{\text{blocking}}}{\overline{\Delta}_{\text{ARQ}}^{\text{preemption}}} \propto \frac{(1-\varepsilon(1-\lambda))(1-\varepsilon \mathrm{e}^{-2\alpha})}{(1-\varepsilon)(1-\varepsilon(1-\lambda)\mathrm{e}^{-2\alpha})} > 1, \forall \lambda, \mathsf{snr}. \tag{2.93}$$

We also obtain

$$\frac{\overline{\Delta}_{\text{HARQ}}^{\text{blocking}}}{\overline{\Delta}_{\text{HARQ}}^{\text{preemption}}} \propto \frac{\mathrm{e}^{\theta \mathrm{e}^{-2\alpha}}(1-\mathrm{e}^{-2\alpha-\theta(1-\mathrm{e}^{-2\alpha})})(1-\mathrm{e}^{-2\alpha}(1-\mathrm{e}^{-\theta}))}{(1+\theta)(1-\mathrm{e}^{-2\alpha})},$$

which, after the analysis similar to the one shown in (2.89) indicates that the blocking may be preferred over preemption in some system setups of α, λ and snr.

In particular:

$$\exists \hat{\alpha}, \forall \alpha > \hat{\alpha} \quad \frac{\overline{\Delta}_{\text{HARQ}}^{\text{blocking}}}{\overline{\Delta}_{\text{HARQ}}^{\text{preemption}}} > 1, \tag{2.94}$$

i.e., for sufficiently large α, the preemption policy should be preferred over blocking. This is because the correlation between the received samples, decreases with α and then, the fresh packets

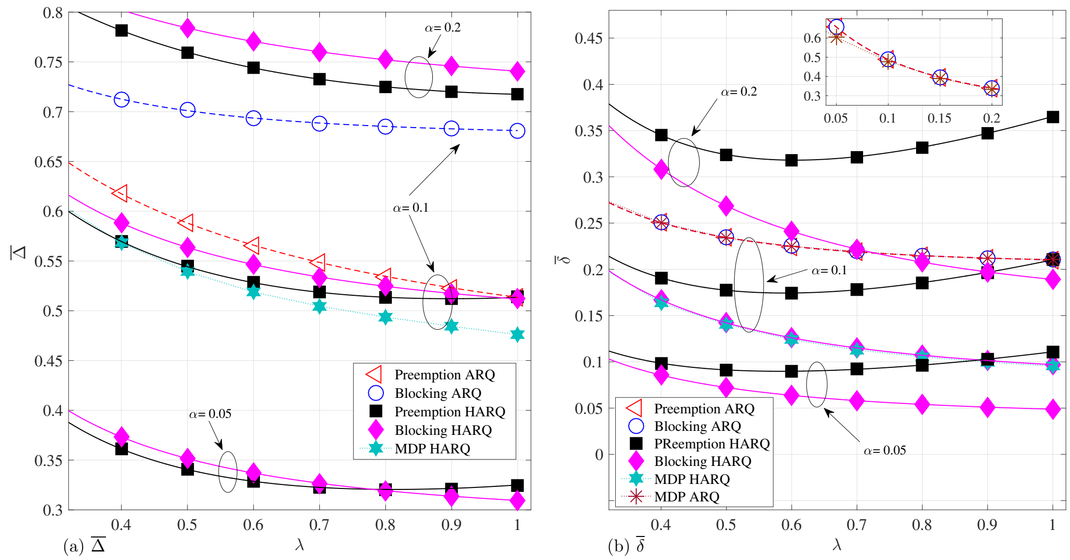

Figure 2.3: a) $\overline{\Delta}$ vs λ and b) $\overline{\delta}$ vs λ, for OU process with $\mathsf{snr} = -3$dB and $\alpha = 0.1$ for ARQ and $\alpha = 0.05, 0.1, 0.2$ for HARQ; Monte-Carlo simulations (markers) and analytical results (lines).

decrease the estimation error. This phenomenon is illustrated in Fig. 2.3 where we show the results for different values of α.

For completeness, we also show the results of the non-causal distortion in Fig. 2.3. The results are qualitatively similar to those obtained for the average causal distortion. In particular, for HARQ, the relationship (2.90) holds as can be found from (2.62) and (C.4). We can also appreciate that $\overline{\delta}$ is much smaller than $\overline{\Delta}$.

Optimal Policies

The MDP solution is also shown in Fig. 2.3 for $\mathsf{snr} = -3$dB and for $\alpha = 0.1$. From the figure, it is clear that the optimal policy must be a mixture of preemption and blocking actions in both causal and non-causal estimations. Further, we plot Fig. 2.4 to show how the optimal actions in non-causal and causal estimations are different for a system under HARQ scheme. This figure shows the optimal policies for each state $(\Delta, d, 1)$ in a causal and non-causal estimations under the same setup of $\lambda = 0.4$, $\alpha = 0.1$ and $\mathsf{snr} = -3$dB. We can observe that the optimal policy follows mostly blocking in non-causal while it follows preemption in causal strategy. Moreover, the behaviour of non-causal distortion in OU is similar to the Wiener model, independently of the α value setup,

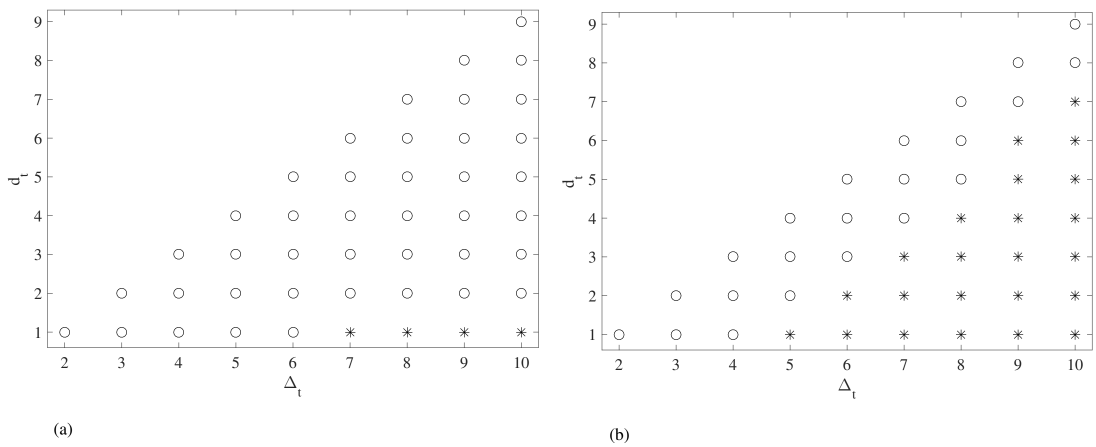

Figure 2.4: The optimal policies for minimizing a) $\overline{\delta}$ and b) $\overline{\Delta}$ under HARQ with $\lambda = 0.4$, $\mathsf{snr} = -3$dB and $\alpha = 0.1$; stars represent preemption, and circles represent blocking.

always blocking is better than preemption.

Effect of Mismatch Model

We will analyze the impact of the model mismatch on the estimation error. Namely, the causal and non-causal estimation strategy based on the Wiener model will be applied when the source signal is a colored Gaussian noise; we will be able to elucidate the impact of the mismatch by varying the correlation $\kappa = \mathrm{e}^{-\alpha}$.

This effect will be evaluated through the simulation by using the relative excess average error defined for the causal distortion as well as for the non-causal distortion, respectively:

$$\Xi = \frac{\overline{\tilde{\Delta}} - \overline{\Delta}}{\overline{\Delta}}, \tag{2.95}$$

$$\xi = \frac{\overline{\tilde{\delta}} - \overline{\delta}}{\overline{\delta}}. \tag{2.96}$$

We will focus on the particular case of low SNR (-3dB), where the differences between the

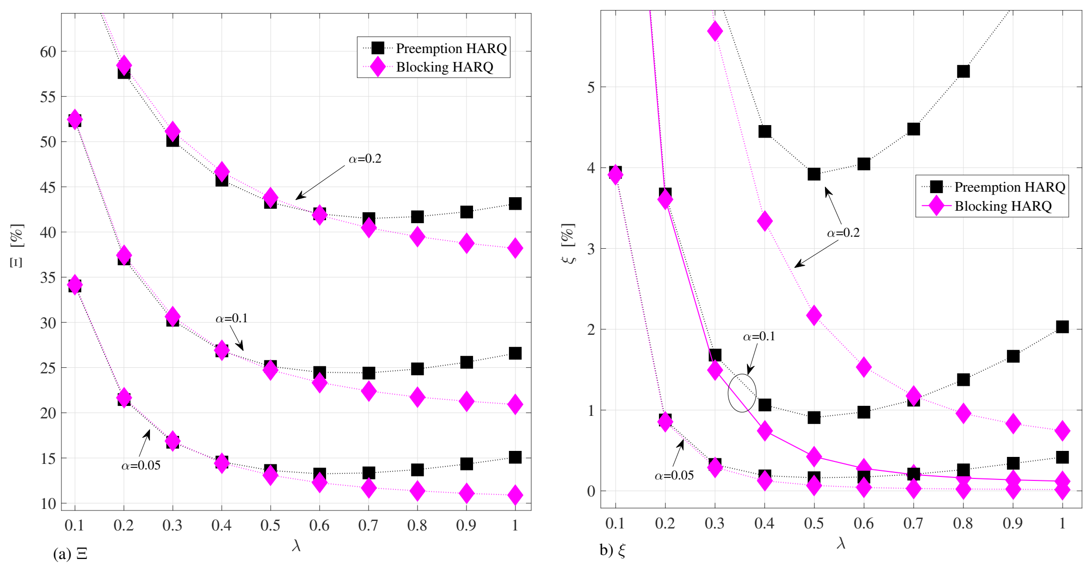

Figure 2.5: Relative increase of the a) average causal distortion, Ξ and b) average non-causal distortion, ξ , for $\mathsf{snr} = -3$dB and $\alpha = 0.05, 0.1, 0.2$; Monte-Carlo simulations (markers).

estimation methods and buffer management policies are the most notorious and we conclude, see Fig. 2.5 :

- The relative increase of the average causal distortion, Ξ, is significantly more important than the corresponding increase of ξ. The non-causal estimation is thus more robust towards the model mismatch.
- With the increased correlation (low α) the model mismatch is much less important and the linear interpolation strategies based on the Wiener model may provide satisfactory solution. This is particularly notable for the non-causal estimation where, despite the mismatch, the value of ξ is measured in fractions of one percent.

2.6 Conclusion

In this chapter we formulated the concept of information semantic for non-real time sensor networks. We presented the study on how to formulate and define the evaluation of the quality of available information in the monitor. We assumed that the variance of the estimation error is a meaningful evaluation criterion, which is indeed the case when dealing with the Markovian Gaussian process. Then we looked into the role of the signal model at the sensor, the importance of the optimal estimation strategy at the monitor, as well as the impact of the sub-optimal estimation incurred by the model mismatch.

In particular:

- We showed that with the Markovian Gaussian process model, the alternative estimation strategy at the monitor may be non-causal and the corresponding criterion changes significantly comparing to the causal estimation.

- The non-causal estimation, should be considered as a viable approach in the monitoring application when the real-time estimation is not required. When compared to the causal estimation, the main advantage of non-causal approach, is that it produces significantly lower variance of the error and is much less sensitive to the model mismatch. The latter may be particularly important as the knowledge of the model or its estimation may be very hard in the real-world applications.

- We have shown that in the simple case of the ARQ it is possible to draw clear-cut conclusions about the optimal buffer management strategies. Other cases are much more complex and we show that notable improvement may be obtained by adaptive policies (obtained by the MDP optimization).

Last, we indicate that while the approach we adopted and which takes into account the model of the measurement signal at the source goes beyond the limitation of the conventional communication-theoretic analysis, it has its own limitations. In particular, we considered the simplest random sampling strategy at the sensor; removing this simplification requires more involved analysis. Similarly, the possibility of optimal estimation at the monitor hinges on the knowledge of the source model, thus the estimation of the model's parameters from the randomly arriving samples is another challenge. While we (partially) addressed this issue considering the mismatched-model estimation (via linear interpolation), there is clearly room for further improvement and analysis.

Chapter 3

Real Time Status Updates in Wireless HARQ with Imperfect Feedback Channel

This chapter investigate the impact of a noisy environment on the performance of the semantic communication system. To evaluate this impact, we use the recently introduced metric, AoI. AoI metric can quantify the timely access of the controller (monitor) to the sensed data in the user side. Thus, the contribution of all the system elements affecting the delivery time is captured in a single metric, the AoI.

In a real practical communication, a wireless channel is erroneous and data packets are at risk of being lost before being decoded fully at the receiver. In order to provide a balance between the delay and the reliability, both affecting the transmission timeliness that may be captured by the AoI, re-transmission techniques are widely applied over data packet transmissions [48]. Conventionally, re-transmission schemes including ARQ and HARQ are used to ensure the reliable transmission over error-prone channels by allowing multiple transmission rounds of the same data [43]. It presumes that the feedback between the communicating parties is established allowing them to decide whether the re-transmission is necessary or not based on the received acknowledgment which is either ACK or NACK. In a way, it trade-offs the delay and reliability according to the predefined constraints on one or another.

To model and analyse this problem, We consider a point-to-point communication setup employing packet combining strategies to transmit status update packets over an erroneous wireless data channel. The sender receives the ACK or NACK of packet reception over an error-prone wireless feedback channel. To detect and control the errors in the feedback channel, we assume a BAC model in the sensor side. Then, we compute the explicit expressions for the Average Age of Information (AAoI) under two fixed policies called preemptive and non-preemptive. Moreover, we show the long term performance of AoI under optimum parameter design of the control channel model.

The remainder of the paper is organized as follows. The buffer management policy, the proposed data forward channel and control feedback channel models, and the formal definition of the AoI are presented in details in Sec. 3.1. Sec. 3.2 computes the closed form expressions for AAoI under preemptive queue with ARQ and HARQ transmission schemes. The same transmission strategies are studied under non-preemptive queue policy in Sec. 3.3. Finally, Sec. 3.4 shows the numerical examples and that the theoretical results match the numerical simulations. Conclusions are provided in Sec. 3.5.

3.1 System Model

We consider a *sensor* communicating its status to a *monitor* through an erroneous wireless forward channel and receiving its acknowledgment through a noisy wireless control channel. Time is organized in equal-length frames covering the round trip time which includes the transmission of data symbols and reception of the ACK or NACK feedback messages carried in the feedback control channel. After receiving a NACK, the sensor transmits another copy of the packet in the next round until an ACK message receive. Re-transmissions can take infinite numbers due to implementing the infinite HARQ protocol scheme. In the following subsections the forward data channel and feedback control channel models will be discussed.

The inter-departure time of the status update packet process in the sensor side assumes to follow a geometric distribution; that is, at the beginning of every time slot, a new update packet may be produced with probability λ. Thus, the probability of having a new generated packet in the buffer r

time slots after the last arrived packet in the buffer is

$$p_R(r) = (1-\lambda)^{r-1}\lambda, \quad r = 1, 2, \dots \tag{3.1}$$

Moreover, the sensor maintains a buffer of one packet capacity which leads the sensor to either drop the current packet under service according to a preemptive policy or drop the new generated status packet at each time slot in case of non-preemptive queue management.

3.1.1 Forward Transmission Channel Model

Applying re-transmission schemes, each status packet will be transmitted in infinite number of rounds until a positive acknowledgement is detected at the sensor. Then, the signal $\mathbf{y}_d^{(k)}$ received at the monitor in round k is modelled as [43, 44]

$$\mathbf{y}_d^{(k)} = \sqrt{\phi_d^{(k)}}\,\mathbf{x_d} + \mathbf{z}_d^{(k)}, \quad k = 1, 2, \dots, \tag{3.2}$$

where $\mathbf{x}_d$ is the input symbols drawn from unit-variance, zero-mean constellation, $\mathbf{z}_d^{(k)}$ denotes (the sequence of) the Gaussian noise modeled with $\mathbf{z}_d \sim \mathcal{N}(0, 1)$. The variable $\phi_d^{(k)}$ is the data channel SNR experienced by the monitor in round k which is assumed to be completely known at the receiver while unknown at the transmitter. Considering the block-fading Rayleigh model, the realization of random variable ϕ_d follows an exponential distribution

$$p_{\mathsf{SNR}}(\phi_d) = \frac{1}{\mathsf{snr}_d}\exp\Big(-\frac{\phi_d}{\mathsf{snr}_d}\Big), \tag{3.3}$$

where snr_d is the average SNR in the forward channel. We further assume that the SNR variable at each slot is is independent and identical from other slots.

As for the re-transmission scheme, two different methods to deal with the received signal at the monitor are considered; namely, ARQ and HARQ. In ARQ, the monitor simply decodes the latest transmission in each round k. While in HARQ the set of all previously received signals must be used to decode the signal at each round. Consequently, we can define the packet decoding error by conditioning on the value of the mutual information function of the SNR [43, 44]

$$\mathsf{NACK}_k \triangleq \begin{cases} \{I(\phi_d^{(k)}) < \rho\} & \text{ARQ} \\ \left\{I\left(\sum_{l=1}^{k} \phi_d^{(l)}\right) < \rho\right\} & \text{HARQ}, \end{cases} \tag{3.4}$$

where ρ is the nominal transmission rate and $I(a) = \log_2(1+a)$, that is, we assume that the Shannon limit for the encoding-decoding scheme is attainable. Since the decoding errors are attributed to the random variation of the SNR as modeled in (3.3), we can write the distribution of the probability of packet decoding error at k-th transmission round, $p_F(k) \triangleq \Pr\{\mathsf{NACK}_k\}$,as follows

$$p_F(k) = \begin{cases} \varepsilon^k & \text{ARQ} \\ \gamma(\theta, k+1) & \text{HARQ}, \end{cases} \tag{3.5}$$

Where $\varepsilon = 1 - \mathrm{e}^{-\theta}$ and $\theta = (2^{\rho} - 1)/\mathsf{snr}_d$. Moreover, $\gamma(\theta, k)$ denotes the regularized lower incomplete gamma function defined as $\gamma(a,b) = \frac{1}{(b-1)!}\int_0^a x^{b-1} e^{-x}\, dx$.

The probability of successful decoding a packet in the kth re-transmission round can be further computed via $p_S(k) = p_F(k-1) - p_F(k)$, where $p_S(k) \triangleq \Pr\{\mathsf{ACK}_k\}$. Then, from (3.5), we can calculate the probability distribution of the required number of frames to completely decode a status packet at the receiver by

$$p_S(k) = \begin{cases} (1-\varepsilon)^{k-1}\varepsilon & \text{ARQ} \\ \frac{\theta^{(k-1)}}{(k-1)!}\mathrm{e}^{-\theta} & \text{HARQ}, \end{cases} \tag{3.6}$$

which are *Geometric* and *Poisson* distributions with parameters $(1-\varepsilon)$ and (θ).

3.1.2 Feedback Transmission Channel Model

The message conveyed by the feedback signal updates the sensor about the success or failure in decoding the last received packet in the monitor. We assume that the feedback and froward channels are independent and adopt the same channel model as in the forward link to model the output signal

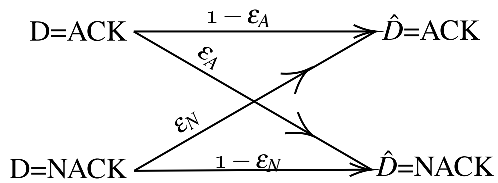

Figure 3.1: BAC model for the acknowledgement detection in the feedback channel

from the control channel at the sensor side

$$\mathbf{y}_c^{(k)} = \sqrt{\phi_c^{(k)}}\,\mathbf{x}_c + \mathbf{z}_c^{(k)}, \quad k = 1, 2, \ldots \tag{3.7}$$

where $\mathbf{x}_c$ is a one bit data packet encoded using a BPSK modulation to carry the ACK/NACK result which is $\mathbf{x}_c = +1$ in case ACK is raised and $\mathbf{x}_c = -1$ otherwise. Besides, the distribution of SNR is assumed to follow exponential form of a Rayleigh fading model provided in (3.3) with the known average SNR of snr_c.

From the normal distribution of variable $\mathbf{z}_c^{(k)}$, we can show the probability distribution of the received signal at the sensor side as:

$$p(y_c|a) = \frac{1}{\sqrt{2\pi}} e^{-\frac{(y_c - a)^2}{2}} \tag{3.8}$$

where $a = +\sqrt{\phi_c}$ if an ACK is raised and $a = -\sqrt{\phi_c}$ otherwise.

Considering the one bit acknowledgement which is carried in the ACK/NACK feedback procedure ($D_k \in \{A, N\}$), we can model the feedback channel with a BAC model as shown in Fig. 3.1. Knowing that the feedback messages are independent at each round, a binary detection procedure must be applied to detect the ACK/NACK response upon reception of the acknowledgement packet at the sensor. Accordingly, at each time, the received signal from (3.7) will be compared with a pre-defined threshold, Θ, to detect an ACK if $y_k > \Theta$ and a NACK otherwise. Hence, the detection outcome $\hat{D}_k \in \{A, N\}$ is defined as:

$$\hat{D}_k = \begin{cases} N \Leftrightarrow y_k \leq \Theta \\ A \Leftrightarrow y_k > \Theta \end{cases} \tag{3.9}$$

From the conditional Gaussian distribution in (3.8) and the detection strategy provided in (3.9), one can show that the probability of undetected ACK message at each round is equal to:

$$\varepsilon_A = p(\hat{D} = N | D = A) = \mathbb{E}_{\mathsf{SNR}}[Q(\sqrt{\phi_c} - \Theta)] \tag{3.10}$$

and the probability of a NACK miss-classification as an ACK is

$$\varepsilon_N = p(\hat{D} = A | D = N) = \mathbb{E}_{\mathsf{SNR}}[Q(\sqrt{\phi_c} + \Theta)] \tag{3.11}$$

where $Q(.)$ denotes the Q-function. Clearly, from the aforementioned ACK and NACK detection method, positive values of Θ will assign ACK signals higher probability of being detected correctly compared to the NACK signals ($\varepsilon_N > \varepsilon_A$).

3.1.3 Definition of Average AoI

AoI is a discrete random process defined by the number of time frames elapsed since the last successfully decoded packet was generated. Let $\Lambda(\tau)$ and $\Omega(\tau)$ be respectively the arrival time (at the monitor) and the generation time (at the sensor) of the τ-th successfully decoded packet. Then, the AoI at time frame t is calculated as [29]

$$\Delta(t) \triangleq t - \Omega\big(\hat{\tau}(t)\big) \quad t = 1, 2, \dots \tag{3.12}$$

where $\hat{\tau}(t)$ is the index of the most recent successfully decoded packet before time t, $\hat{\tau}(t) = \max\{\tau : \Lambda(\tau) \leq t\}$.

To capture the quality of the information the monitor obtains from the sensor, the long-term AAoI is used [29, Sec. 3-4, (3-25)]

$$\overline{\Delta} = \frac{\mathbb{E}_X[X^2]}{2\,\mathbb{E}_X[X]} + \mathbb{E}_Y[Y] - \frac{1}{2}, \tag{3.13}$$

where Y is the effective transmission time of a successfully decoded packet in the monitor which is defined as the required number of time slots to accomplish the transmission of a status update

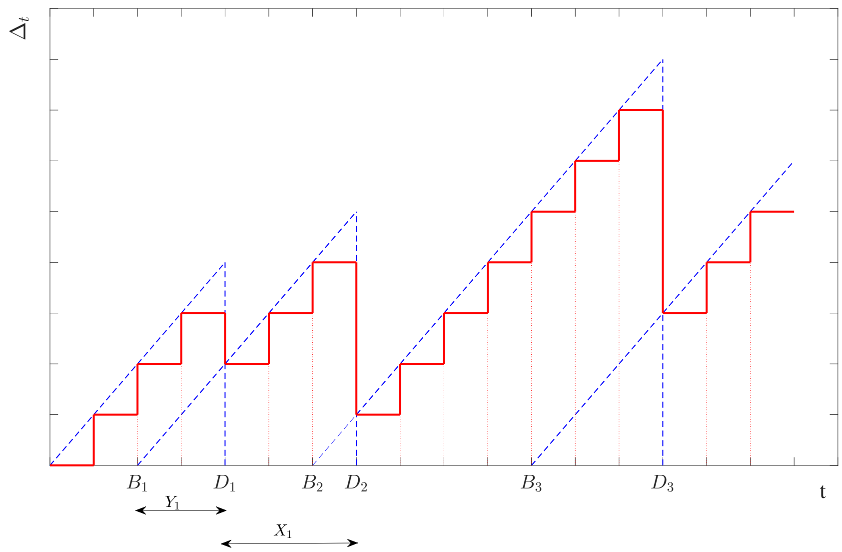

Figure 3.2: Evolution of AoI

packet. Besides, X represents the inter-departure time of the successfully decoded packets at the monitor. A sample path of AoI is plotted in 3.2. The time duration of X and Y are shown for the first renewal period.

3.1.4 Definition of Average Channel Utilization

The channel utilization, (η), denotes the fraction of time a sensor is busy (in transmission) until a successful transmission occurs. To calculate the expected of η, we define discrete-time renewal chain where the channel occupancy is a binary variable taking value of one when the transmission is taking place, and zero when the sensor is not transmitting. The average channel utilization, ($\overline{\eta}$), is then calculated directly as

$$\overline{\eta} = \lim_{N\to\infty} \frac{(C_1+O_1)+\ldots+(C_N+O_N)}{X_1+\ldots+X_N} = \frac{\mathbb{E}[C]+\mathbb{E}[O]}{\mathbb{E}[X]}, \tag{3.14}$$

where C and O are the time the sensor is busy with transmission of successfully and unsuccessfully decoded packets between two successive successfully decoded packets in the monitor.

In what follows, each section presents in detail the derivations to describe the AAoI and the channel utilization for the introduced buffer management policies including *preemptive* and *non-preemptive* queue.

3.2 AAoI analysis under preemptive queue

In this section, we assume a preemptive management policy in which any new generated packet truncates the transmission of the packet under service and start its transmission immediately. In what follows, we present the arguments to calculate the AAoI equation. To evaluate the AAoI in (3.13), we need first to compute the inter-departure time of the successfully decoded status packets, X. We note that only the set of completely decoded packets can provide new information and thus reduce the age value. In other words, the status packets which fail to deliver at the monitor will impact the renewal period and therefore will affect X duration. In order to derive the exact distribution and moments of X, we need to decompose the inter-departure time to the possible events may happen during this time period.

According to the introduced system setup, we know that a packet under service may leave the buffer before completing its transmission either if a new status packet preempts its service or if a NACK miss-detection occurs during its re-transmission rounds. therefore, between two decoded packets at the monitor, a set of packets (N) might be preempted each taking a random duration of A time slots and a second set of packets (M) might be dropped due to the NACK miss-classification each taking B time slots. Consequently, X can be decomposed as

$$X = Y + I + \sum_{i=0}^{N} A_i + \sum_{j=0}^{M} (B_j + I_j) \tag{3.15}$$

where the variable I in the summations is the waiting time to receive a new update packet once a packet under service departs the system. Since the arrival process is geometric and hence memory-less, we deduce that the waiting time I is geometric distributed with parameter (λ). Therefore, the probability of the system to be idle for k time slots is given by

$$I_k = \lambda(1-\lambda)^k,\ k = 0, 1, \ldots \tag{3.16}$$

From the decomposition in (3.15) and the independence of the decomposed elements, we can write the first moment of X as follows

$$\mathbb{E}[X] = \mathbb{E}[Y] + (\mathbb{E}[M] + 1)\,\mathbb{E}[I] + \mathbb{E}[N]\,\mathbb{E}[A] + \mathbb{E}[M]\,\mathbb{E}[B] \tag{3.17}$$

and the second moment of X can be expressed as

$$\begin{aligned}\mathbb{E}[X^2] = {} & \mathbb{E}[Y^2] + \mathbb{E}[I^2] + \mathbb{E}[A]^2\,\mathbb{E}[N^2] + 2\,\mathbb{E}[Y]\,\mathbb{E}[I] \\ & + \mathbb{E}[N](\mathrm{Var}[A] + 2\,\mathbb{E}[A]\,\mathbb{E}[Y] + 2\,\mathbb{E}[A]\,\mathbb{E}[I]) \\ & + \mathbb{E}[M](\mathrm{Var}[B] + \mathrm{Var}[I] + 2(\mathbb{E}[Y] + \mathbb{E}[I])(\mathbb{E}[B] + \mathbb{E}[I])) \\ & + (\mathbb{E}[B] + \mathbb{E}[I])(\mathbb{E}[M^2](\mathbb{E}[B] + \mathbb{E}[I]) + 4\,\mathbb{E}[N]\,\mathbb{E}[M]\,\mathbb{E}[A])\end{aligned} \tag{3.18}$$

At this stage, we need to evaluate the moments of the elements in the decomposition to be able to determine the AAoI under the preemption policy. First, we start by evaluating the probability distribution of A and B.

***Lemma* 3.2.1.** *The probability distribution function of variables A and B are given by:*

$$p_A(k) = p_B(k) = \begin{cases} (1-\varepsilon(1-\varepsilon_N)(1-\lambda))(\varepsilon(1-\varepsilon_N)(1-\lambda))^{k-1} & \textit{ARQ} \\ \frac{1-(1-\varepsilon_N)(1-\lambda)}{1-e^{-\theta(1-(1-\lambda)(1-\varepsilon_N))}}\gamma(\theta,k)((1-\varepsilon_N)(1-\lambda))^{k-1} & \textit{HARQ} \end{cases} \tag{3.19}$$

Proof. See Appendix E. □

Using the derived probability distribution in (3.19), we have the first two moments of A and B:

$$\mathbb{E}[A] = \mathbb{E}[B] = \begin{cases} \frac{1}{1-\varepsilon(1-\varepsilon_N)(1-\lambda)} & \text{ARQ} \\ \frac{1-e^{-\theta(1-\varphi)}(1+\theta\varphi(1-\varphi))}{(1-\varphi)(1-e^{-\theta(1-\varphi)})} & \text{HARQ} \end{cases} \tag{3.20}$$

$$\mathbb{E}[A^2] = \mathbb{E}[B^2] = \begin{cases} \frac{1+\varepsilon(1-\varepsilon_N)(1-\lambda)}{(1-\varepsilon(1-\varepsilon_N)(1-\lambda))^2} & \text{ARQ} \\ \frac{\theta\varphi(1-\varphi+\theta\varphi(1-\varphi)+2)}{(1-\varphi)(1-e^{\theta(1-\varphi)})} + \frac{1+\varphi}{(1-\varphi)^2} & \text{HARQ} \end{cases} \tag{3.21}$$

where $\varphi = (1-\lambda)(1-\varepsilon_N)$. Furthermore, we can derive the variance of A and B by substituting (3.20) and (3.21) into the relation of $\mathrm{Var}[A] = \mathbb{E}[A^2] - \mathbb{E}[A]^2$.

Now, we need to compute the number of packet failures due to the preemption (N) and NACK miss-detection (M). Let P_Ψ denotes the probability of packet failure due to the preemption event and P_Υ due to the NACK miss-classification. therefore, the total number of dropped packets shown by L in every renewal will be geometric distributed with parameter $(1-(P_\Psi + P_\Upsilon))$. Then, the probability distribution of the N number of dropped packets out of the total of L dropped ones is

$$p_N(k) = (\frac{P_\Psi}{1-P_\Upsilon})^k \frac{1-(P_\Psi + P_\Upsilon)}{1-P_\Upsilon} \tag{3.22}$$

and similarly the distribution of M can be written as

$$p_M(k) = (\frac{P_\Upsilon}{1-P_\Psi})^k \frac{1-(P_\Psi + P_\Upsilon)}{1-P_\Psi} \tag{3.23}$$

We further need to describe and calculate the probabilities of P_Ψ and P_Υ. Let $\hat{D}_{1:k} = [\hat{D}_1, ..., \hat{D}_k]$ contains the sequence of detection outcomes on the feedback channel up to round k. Then, from the independence of the status packet generation process (R) in (3.1), packet transmission completion time (S) in (3.6) and the detection of the feedback value in (3.9), the probability of P_Ψ can be obtained:

$$\begin{aligned} P_\Psi &= \Pr\{(S > R), (\hat{D}_{1:R} = N | D_{1:R} = N)\} \\ &= \sum_{k=1}^{\infty} p_R(k) \left(\Pr\{S > k\} \Pr\{\hat{D}_{1:k} = N | D_{1:k} = N\}\right) \\ &= \sum_{k=1}^{\infty} p_R(k) \sum_{j=k}^{\infty} p_S(j) \prod_{i=1}^{k} p(\hat{D}_i = N | D_i = N) \\ &= \begin{cases} \frac{\lambda(1-\varepsilon_N)\varepsilon}{1-(1-\lambda)(1-\varepsilon_N)\varepsilon} & \text{ARQ} \\ \frac{\lambda(1-\varepsilon_N)}{1-\varphi}(1-e^{-\theta(1-\varphi)}) & \text{HARQ,} \end{cases} \end{aligned} \tag{3.24}$$

where the probability term $p(\hat{D}_{1:k} = N | D_{1:k} = N)$ assures that the NACK messages are correctly detected so that the old packet will stay under service until a new status update arrives at the buffer and preempt its service process, which is reflected in the probability term $\Pr\{S > R\}$. Note that, the last term in (3.24) is obtained by exploiting (3.1), (3.6) and (3.11).

Similarly, we can quantify the packet transmission failure probability due to the event of NACK miss-classification denoted by P_Υ. Independence of status update packet arrival process, packet completion time in (3.5) and the feedback signal detection provides that

$$\begin{aligned} P_\Upsilon &= \Pr\{(R \geq F), (\hat{D}_{1:F-1} = N, \hat{D}_F = A | D_{1:F} = N)\} \\ &= \sum_{k=1}^{\infty} p_F(k) \left(\Pr\{R \geq k\} \Pr\{\hat{D}_{1:k-1} = N, \hat{D}_k = A | D_{1:k} = N\} \right) \\ &= \sum_{k=1}^{\infty} p_F(k) \sum_{j=k}^{\infty} p_R(j) p(\hat{D}_k = A | D_k = N) \prod_{i=1}^{k-1} p(\hat{D}_i = N | D_i = N) \\ &= \begin{cases} \frac{\varepsilon \varepsilon_N}{1-\varepsilon(1-\varepsilon_N)(1-\lambda)} & \text{ARQ} \\ \frac{\varepsilon_N}{1-(1-\lambda)(1-\varepsilon_N)} (1 - e^{-\theta(1-(1-\lambda)(1-\varepsilon_N))}) & \text{HARQ}, \end{cases} \end{aligned} \tag{3.25}$$

where the term $\Pr\{\hat{D}_{1:k-1} = N, \hat{D}_k = A | D_{1:k} = N\}$ represents that the packet under service truncates its re-transmission rounds once the NACK message is miss-detected as an ACK. Moreover, the relation $\Pr\{R \geq F\}$ guarantees that no new packet preempts the re-transmissions before a miss-detection happens.

Then, substituting (3.24)-(3.25) into the (3.22)-(3.23), it is readily to evaluate the expected value of the random number of N as in the following

$$\mathbb{E}[N] = \begin{cases} \frac{\lambda\varepsilon(1-\varepsilon_N)}{1-\varepsilon} & \text{ARQ} \\ \frac{\lambda(1-\varepsilon_N)(e^{\theta(1-\varphi)}-1)}{1-\varphi} & \text{HARQ}, \end{cases} \tag{3.26}$$

and the expected value of variable M as

$$\mathbb{E}[M] = \begin{cases} \frac{\varepsilon\varepsilon_N}{1-\varepsilon} & \text{ARQ} \\ \frac{\varepsilon_N(e^{\theta(1-\varphi)}-1)}{1-\varphi} & \text{HARQ}, \end{cases} \tag{3.27}$$

further, the second moments will be obtained from $\mathbb{E}[N^2] = 2\mathbb{E}^2[N] + \mathbb{E}[N]$ and $\mathbb{E}[M^2] = 2\mathbb{E}^2[M] +$

$\mathbb{E}[M]$.

Lastly, we need to derive the probability distribution function of the effective service time of the successfully delivered packets (Y). A packet entered the system can fulfil its service provided that it is not preempted by the next generated status packet and not truncates its re-transmissions due to the erroneously detected NACK messages as ACK. Hence,

$$p_Y(k) = \Pr\{S = k|(R > S), (\hat{D}_{1:S-1} = N|D_{1:S-1} = N)\} \tag{3.28}$$

From the independence of status packet arrivals and feedback message detection process, we find that the distribution of Y follows the same distributions as in (3.6) with new parameters of $\varepsilon(1-\lambda)(1-\varepsilon_N)$ in ARQ and $\theta(1-\lambda)(1-\varepsilon_N)$ in HARQ. Therefore the first two moments are given by

$$\mathbb{E}[Y] = \begin{cases} \frac{1}{1-\varepsilon(1-\varepsilon_N)(1-\lambda)} & \text{ARQ} \\ 1+\theta(1-\varepsilon_N)(1-\lambda) & \text{HARQ} \end{cases} \tag{3.29}$$

and,

$$\mathbb{E}[Y^2] = \begin{cases} \frac{1+\varepsilon(1-\varepsilon_N)(1-\lambda)}{(1-\varepsilon(1-\varepsilon_N)(1-\lambda))^2} & \text{ARQ} \\ 1+3(\theta\varphi)+(\theta\varphi)^2 & \text{HARQ} \end{cases} \tag{3.30}$$

We can now express the closed-form expressions of (3.17) and (3.18) by using the moment terms derived above. By substituting the obtained relations in (3.20), (3.26), (3.27) and (3.29) into (3.17), and after some simplifications, we get

$$\mathbb{E}[X] = \begin{cases} \frac{1-\varepsilon(1-\varepsilon_N)(1-\lambda)}{\lambda(1-\varepsilon)} & \text{ARQ} \\ \frac{e^{\theta(1-\varphi)}}{\lambda} & \text{HARQ,} \end{cases} \tag{3.31}$$

Further, the expression of the second moment of X can be derived for ARQ as

$$\mathbb{E}_{\text{ARQ}}[X^2] = \frac{1+\varepsilon}{(1-\varepsilon)^2} + \frac{2\lambda(1-\lambda)\varepsilon\varepsilon_N}{(1-\varepsilon)^2\lambda} + \frac{(1-\lambda)(1-\varepsilon(1-\varepsilon_N))}{(1-\varepsilon)^2\lambda^2}$$

$$+(\lambda(1-\varepsilon)+2(1-\varepsilon(1-\varepsilon_N)(1-\lambda))) \tag{3.32}$$

and for the case of HARQ, we have

$$\begin{aligned}\mathbb{E}_{\text{HARQ}}[X^2] &= (e^{\theta(1-\varphi)}-1)\,\mathbb{E}[A^2]+(1+\theta\varphi)^2+\theta\varphi \\ &+2\,\mathbb{E}[A](e^{\theta(1-\varphi)}-1)\left(\frac{\lambda-\varphi e^{-\theta(1-\varphi)}+(1-\lambda)(e^{-\theta(1-\varphi)}(1-\varepsilon_N)+2\varepsilon_N)}{e^{-\theta(1-\varphi)}(1-\varphi)\lambda}\right) \\ &+\frac{1-\lambda}{\lambda}\left(1+\frac{\varepsilon_N(e^{\theta(1-\varphi)}-1)}{1-\varphi}\right)\left(\frac{2-\lambda}{\lambda}+2\left(1+\theta\varphi+\frac{\varepsilon_N(1-\lambda)(e^{\theta(1-\varphi)}-1)}{\lambda(1-\varphi)}\right)\right)\end{aligned} \tag{3.33}$$

Having obtained the closed-form relations for the moments of inter-renewal time (X) and the expected value of Y, we can write the final AAoI expression

$$\overline{\Delta}=\begin{cases}\frac{(1-\varepsilon(1-\varepsilon_N)(1-\lambda))}{\lambda(1-\varepsilon)} & \text{ARQ}\\ \frac{e^{\theta(1-\varphi)}}{\lambda} & \text{HARQ}\end{cases} \tag{3.34}$$

Remark 3.2.1. *The achievable average AoI with preemption in the case that the feedback channel is error-free, i.e., $\overline{\mathsf{snr}}_c \to \infty$, can be expressed as*

$$\overline{\Delta}_\infty=\begin{cases}\frac{2(1-\varepsilon)+\lambda(1+\varepsilon)}{2\lambda(1-\varepsilon)}-\frac{1}{2} & \textit{ARQ}\\ \frac{\mathrm{e}^{\theta\lambda}}{\lambda} & \textit{HARQ}\end{cases} \tag{3.35}$$

The attained $\overline{\Delta}_\infty$ in (3.35) is the optimum average AoI for the preemption policy since it can be shown that it performs as a lower bound for the $\overline{\Delta}$ equation in (3.34). The condition of snr_c can be modeled by pushing the detection threshold Θ to the positive infinite region that can provide $\varepsilon_N=0$ and $\varepsilon_A \leq 1$. Such a detection channel is formally called a Z-Channel since all NACK messages can be detected correctly and miss-classification errors only exist for ACK messages.

At last, we evaluate the resource utilization under preemptive policy. To this end, we need to derive the probability distributions of variable C and O. From (3.15), we know that the overall transmission time of failed packets in every renewal episode is equal to

$$O = \sum_{i=0}^{N} A_i + \sum_{j=0}^{M} B_j \tag{3.36}$$

Therefore, the expected value of O in preemption can be calculated from (3.20), (3.26) and (3.27) as follows:

$$\mathbb{E}[O] = \begin{cases} \frac{\varepsilon(\lambda(1-\varepsilon_N)+\varepsilon_N)}{(1-\varepsilon_N)^2+\varepsilon(1-\varepsilon)(\lambda(1-\varepsilon_N)+\varepsilon_N)} & \text{ARQ} \\ \frac{(1-e^{\theta(1-\varphi)})(\lambda(1-\varepsilon_N)}{(\varepsilon_N+\lambda(1-\varepsilon_N))^2} & \text{HARQ} \end{cases} \tag{3.37}$$

To calculate the time duration a successfully decoded packet spends in the system since its arrival time into the buffer until its departure time is given by

$$C = Y + I_z \tag{3.38}$$

where I_z is the required time to detect correctly the carried ACK message in the acknowledgment packet as provided in

$$P(I_z = k) = p_R(k)\varepsilon_A^{k+1} + \varepsilon_A^k(1-\varepsilon_A)\Pr\{R \geq k\} = (\varepsilon_A(1-\lambda))^k(1-\varepsilon_A(1-\lambda)) \tag{3.39}$$

with the expected value as

$$\mathbb{E}[I_z] = \frac{\varepsilon_A(1-\lambda)}{1-\varepsilon_A(1-\lambda)} \tag{3.40}$$

From $\mathbb{E}[Y]$ in (3.29) and $\mathbb{E}[I_z]$ in (3.40), we can calculate the moment of C as $\mathbb{E}[C] = \mathbb{E}[Y] + \mathbb{E}[I_z]$. Using the obtained expected value of C and O in (3.37), we can write the average of η as presented in (3.41).

$$\overline{\eta} = \begin{cases} \frac{\varepsilon_A\lambda(1-\lambda)(1-\varepsilon)}{(1-\varepsilon_A(1-\lambda))(1-\varepsilon(1-\varepsilon_N)(1-\lambda))} + \frac{\lambda}{1-\varepsilon(1-\varepsilon_N)(1-\lambda)} & \text{ARQ} \\ e^{-\theta(1-\varphi)}\lambda(1+\theta\varphi+\frac{\varepsilon_A(1-\lambda)}{1-\varepsilon_A(1-\lambda)}) + \frac{\lambda(1-e^{-\theta(1-\varphi)}(1+\theta\varphi(1-\varphi)))}{1-\varphi} & \text{HARQ} \end{cases} \tag{3.41}$$

3.3 AAoI analysis under non-preemptive queue

In this section, we derive the expression for the AAoI in the case that non-preemptive policy manages the queue. Recall that under this policy, a newly arriving packet will be discarded if it finds the system busy. Besides, a packet under service can depart the system only if an ACK is detected at the sensor. Since a NACK may be miss-classified as an ACK, a set of packets may be discarded before completing their transmissions. The inter-departure time, X, will be affected by the aforementioned set of failed packets in between two successive successfully decoded ones. Let L denotes the random number of packet loss in every renewal episode and W represents the random number of time slots every failed status packet occupies. Then, we can decompose the inter-departure time X under non-preemptive policy as follows:

$$X = V + I + \sum_{i=0}^{L}(W_i + I_i) \tag{3.42}$$

where, V represents the time duration which is required to accomplish a successful packet reception at the monitor and I shows the system idle time to receive a new packet once a packet under service leaves the buffer. Since the status packet generation process is memory-less, the distribution of variable I follows the same relation as provided in (3.16).

From (3.42), the first moment is equal to

$$\mathbb{E}[X] = \mathbb{E}[V] + \mathbb{E}[L]\,\mathbb{E}[W] + \mathbb{E}[I](\mathbb{E}[L] + 1) \tag{3.43}$$

and the second moment of X will be

$$\begin{aligned}\mathbb{E}[X^2] = \mathbb{E}[V^2] + \mathbb{E}[W]^2(\mathbb{E}[L^2] - \mathbb{E}[L]) + 2\,\mathbb{E}[V](\mathbb{E}[I] + \mathbb{E}[L](\mathbb{E}[I] + \mathbb{E}[W]))\\ + (\mathbb{E}[L^2] + \mathbb{E}[L])(2\,\mathbb{E}[W]\,\mathbb{E}[I] + \mathbb{E}[I]^2) + \mathbb{E}[L](\mathbb{E}[W^2] + \mathbb{E}[I^2]) + \mathbb{E}[I^2]\end{aligned} \tag{3.44}$$

Therefore, we need to compute the moments of the number of failed packets, L, and time duration each successful and failed packet spent in the system, V and W to be able to find the final expression of AAoI under non-preemptive queue.

First, we start by characterizing the random variable L. Since L represents the number of packet failures before each successful packet transmission, its distribution follows a geometric probability distribution with parameter $(1-P_w)$, where P_w is the probability that a packet under service truncates its re-transmission rounds before completion of its demand service time.

$$p_L(k) = (1-P_w)(P_w)^k \; ; k = 0, 1, ... \tag{3.45}$$

To calculate the packet loss probability, P_w, let Q denote the random number of correct NACK detection before the first miss-detection happens. Simply, we can write this event as a Geometric distribution with the success probability of ε_N derived in (3.11)

$$p_Q(k) = \Pr\{\hat{D}_{1:k-1} = N, \hat{D}_k = A | D_{1:k} = N\} = (1-\varepsilon_N)^{k-1}\varepsilon_N \tag{3.46}$$

From the definition of probability P_w, one can show that P_w equals to the event of $\Pr\{S > Q\}$ which shows the packet completion time from (3.6) takes longer time than the first NACK miss-detection happens in (3.46)

$$P_w = \Pr\{S > Q\} = \sum_{k=1}^{\infty} p_Q(k) \sum_{i=k+1}^{\infty} p_S(i) = \begin{cases} \frac{\varepsilon\varepsilon_N}{1-\varepsilon(1-\varepsilon_N)} & \text{ARQ} \\ 1 - e^{-\theta\varepsilon_N} & \text{HARQ}, \end{cases} \tag{3.47}$$

By simply replacing (3.47) in (3.45), the moment values of variable L can be fully characterized as follows

$$\mathbb{E}[L] = \begin{cases} \frac{\varepsilon\varepsilon_N}{1-\varepsilon} & \text{ARQ} \\ e^{\theta\varepsilon_N}(1-e^{-\theta\varepsilon_N}) & \text{HARQ} \end{cases} \tag{3.48}$$

and

$$\mathbb{E}[L^2] = \begin{cases} \frac{\varepsilon\varepsilon_N(1-\varepsilon(1-2\varepsilon_N))}{(1-\varepsilon)^2} & \text{ARQ} \\ e^{2\theta\varepsilon_N}(1-e^{-\theta\varepsilon_N})(1+\varepsilon_N(1-e^{-\theta\varepsilon_N})) & \text{HARQ} \end{cases} \tag{3.49}$$

Next, we need to define the distribution of V, the random number of time slots each successfully delivered packet stays in the system until completing its re-transmissions and detecting its ACK at the monitor. Let U be the probability distribution of number of ACK miss-detection until detecting it correctly. Since the detection results are independent at each round, the distribution of U will follow a geometric with parameter $(1-\varepsilon_A)$ as:

$$p_U(k) = \varepsilon_A^{k-1}(1-\varepsilon_A)\ ; k = 1, \ldots \tag{3.50}$$

Then, the number of frames required to truncate the transmission of a successfully decoded status packet will be $V = Y + U$. Variable Y is the effective transmission time of a successfully decoded packet term in (3.13). With the blocking policy, the effective packet transmission time is simply $p_Y(k) = \Pr\{S = k | S \leq Q\}$, which is the conditional service time given that no NACK miss-detection occurs during the packet service completion time provided in (3.6). Therefore, the distribution of Y follows the same distribution of S with new parameters as:

$$Y \sim \begin{cases} \text{Geom}(1-\varepsilon(1-\varepsilon_N)) & \text{ARQ} \\ \text{Pois}(\theta(1-\varepsilon_N)) & \text{HARQ}, \end{cases} \tag{3.51}$$

with the following first moment

$$\mathbb{E}[Y] = \begin{cases} \frac{1}{1-\varepsilon(1-\varepsilon_N)} & \text{ARQ} \\ \theta(1-\varepsilon_N)+1 & \text{HARQ} \end{cases} \tag{3.52}$$

Now, due to the independence of Y in (3.51) and U in (3.50), we can apply the convolution in discrete domain and

$$\begin{aligned} p_V(k) &= \Pr\{Y+U = k\} = \sum_{i=1}^{k} p_Y(i) p_U(k-i) \\ &= \begin{cases} \frac{(1-\varepsilon_A)(1-\varepsilon(1-\varepsilon_N))}{\varepsilon(1-\varepsilon_N)-\varepsilon_A}\left((\varepsilon(1-\varepsilon_N))^v - \varepsilon_A^v\right) & \text{ARQ} \\ e^{-\theta(1-\varepsilon_N)} \varepsilon_A^{v-1}(1-\varepsilon_A) t_{v-1}\left(\frac{\theta(1-\varepsilon_N)}{\varepsilon_A}\right) & \text{HARQ}, \end{cases} \end{aligned} \tag{3.53}$$

Further, we can derive the first moment of the process V with regard to its obtained distribution function in (3.53)

$$\mathbb{E}[V] = \begin{cases} \frac{(1-\varepsilon_A)(1-\varepsilon(1-\varepsilon_N))}{\varepsilon(1-\varepsilon_N)-\varepsilon_A}\left(\frac{\varepsilon(1-\varepsilon_N)}{(1-\varepsilon(1-\varepsilon_N))^2} - \frac{\varepsilon_A}{(1-\varepsilon_A)^2}\right) & \text{ARQ} \\ \frac{1+\theta(1-\varepsilon_A)(1-\varepsilon_N)}{1-\varepsilon_A} & \text{HARQ} \end{cases} \tag{3.54}$$

and its second moment as given by

$$\mathbb{E}[V^2] = \begin{cases} \frac{(1-\varepsilon_A)(1-\varepsilon(1-\varepsilon_N))}{\varepsilon(1-\varepsilon_N)-\varepsilon_A}\left(\frac{\varepsilon(1-\varepsilon_N)(1+\varepsilon(1-\varepsilon_N))}{(1-\varepsilon(1-\varepsilon_N))^3} - \frac{\varepsilon_A(1+\varepsilon_A)}{(1-\varepsilon_A)^3}\right) & \text{ARQ} \\ \frac{e^{-\theta\varepsilon_N}}{(1-\varepsilon_A)^2}(1+\varepsilon_A+\theta(1-\varepsilon_N)(1-\varepsilon_A)(3-\varepsilon_A+\theta(1-\varepsilon_N)(1-\varepsilon_A))) & \text{HARQ} \end{cases} \tag{3.55}$$

Last, we need to derive the probability distribution function of the failed packet transmission time shown by W. We know that a packet under service fails under the condition that a NACK miss-detection happens before completion time in (3.6)

$$\begin{aligned} p_W(k) &= \Pr\{Q=k|S>k\} = \frac{1}{P_w} p_Q(k) \sum_{i=k+1}^{\infty} p_S(i) \\ &= \begin{cases} (1-\varepsilon(1-\varepsilon_N))(\varepsilon(1-\varepsilon_N))^{k-1} & \text{ARQ} \\ \frac{\varepsilon_N}{(1-e^{-\theta\varepsilon_N})}\gamma(\theta,w)(1-\varepsilon_N)^{w-1} & \text{HARQ,} \end{cases} \end{aligned} \tag{3.56}$$

with the resulting expected value of:

$$\mathbb{E}[W] = \begin{cases} \frac{1}{1-\varepsilon(1-\varepsilon_N)} & \text{ARQ} \\ \frac{1}{\varepsilon_N(1-e^{-\theta\varepsilon_N})}(1-e^{-\theta\varepsilon_N}(1+\varepsilon_N(1-\varepsilon_N)\theta)) & \text{HARQ} \end{cases} \tag{3.57}$$

and the second moment of:

$$\mathbb{E}[W^2] = \begin{cases} \frac{1+\varepsilon(1-\varepsilon_N)}{(1-\varepsilon(1-\varepsilon_N))^2} & \text{ARQ} \\ \frac{2-\varepsilon_N}{\varepsilon_N^2} + \frac{\theta(1-\varepsilon_N)(2+\varepsilon_N(1+\theta(1-\varepsilon_N)))}{\varepsilon_N(1-e^{\theta\varepsilon_N})} & \text{HARQ} \end{cases} \tag{3.58}$$

Now, with the relations at hand, we are able to write the expected value of X :

$$\mathbb{E}[X] = \begin{cases} \frac{1-\lambda\varepsilon\varepsilon_A-(1-\lambda)(\varepsilon_A+\varepsilon(1-\varepsilon_N)(1-\varepsilon_A))}{\lambda(1-\varepsilon)(1-\varepsilon_A)} & \text{ARQ} \\ e^{\theta\varepsilon_N}\frac{\lambda+\varepsilon_N(1-\lambda)}{\varepsilon_N\lambda} - \frac{1-(\varepsilon_N+\varepsilon_A)}{\varepsilon_N} & \text{HARQ} \end{cases} \tag{3.59}$$

Finally, by placing (3.54)-(3.55) and (3.57)-(3.58) in (3.44), we can evaluate the final equation of $\mathbb{E}[X^2]$ as in

$$\begin{aligned}\mathbb{E}_{ARQ}[X^2] = {} & \frac{\varepsilon\varepsilon_N(1+\varepsilon)}{(1-\varepsilon)^2(1-\varepsilon(1-\varepsilon_N))^2} + \mathbb{E}[V^2] + 2\,\mathbb{E}[V]\frac{(1-\lambda)(1-\varepsilon(1-\varepsilon_N))^2+\lambda\varepsilon\varepsilon_N}{\lambda(1-\varepsilon)(1-\varepsilon(1-\varepsilon_N))} \\ & + \frac{1-\lambda}{\lambda^2(1-\varepsilon)^2}(2\varepsilon\varepsilon_N\lambda(1+\varepsilon-\varepsilon_N)+(1-\varepsilon(1-\varepsilon_N))(1-\varepsilon(1-2\varepsilon_N)))\end{aligned} \tag{3.60}$$

$$\begin{aligned}\mathbb{E}_{HARQ}[X^2] = {} & \mathbb{E}[V^2] + \mathbb{E}[W]^2(1-e^{\theta\varepsilon_N})^2(1+\varepsilon_N) + 2\,\mathbb{E}[V]e^{\theta\varepsilon_N}(\frac{1-\lambda}{\lambda}+\mathbb{E}[W](1-e^{-\theta\varepsilon_N})) \\ & + \frac{1-\lambda}{\lambda}(e^{\theta\varepsilon_N}-1)(2+(1+\varepsilon_N)(e^{\theta\varepsilon_N}-1))(2\,\mathbb{E}[W]+\frac{1-\lambda}{\lambda}) \\ & + \mathbb{E}[W^2](e^{\theta\varepsilon_N}-1) + \frac{(1-\lambda)(2-\lambda)}{\lambda^2}e^{\theta\varepsilon_N}\end{aligned} \tag{3.61}$$

From the obtained moment values, the AAoI under non-preemptive policy can be calculated from (3.59)-(3.61) as

$$\overline{\Delta} = \begin{cases} \frac{\mathbb{E}[X^2]}{2\,\mathbb{E}[X]} + \frac{1}{1-\varepsilon(1-\varepsilon_N)} - \frac{1}{2} & \text{ARQ} \\ \frac{\mathbb{E}[X^2]}{2\,\mathbb{E}[X]} + \theta(1-\varepsilon_N) + \frac{1}{2} & \text{HARQ} \end{cases} \tag{3.62}$$

Remark 3.3.1. *On the case that there is no error in the feedback channel, i.e., $\overline{\mathsf{snr}}_c \to \infty$, the expression for the AAoI can be simplified to*

$$\overline{\Delta}_\infty = \begin{cases} \frac{(1-\varepsilon)^2(1-\lambda)(2-\lambda)-\lambda^2(1-3\varepsilon)+2\lambda(2-2\varepsilon+\varepsilon\lambda)}{2\lambda(1-\varepsilon)(1-\varepsilon(1-\lambda))} - \frac{1}{2} & \textit{ARQ} \\ \frac{\lambda(1+\theta)(2+3\theta\lambda)-\lambda(1-2\theta)+2}{2\lambda(1+\theta\lambda)} - \frac{1}{2} & \textit{HARQ} \end{cases} \tag{3.63}$$

We then derive the expression of $\overline{\eta}$ for non-preemptive queue. For the term C, we have the equality that $C = Y$ since no packet can interrupt the service of an old packet. Next, we have the distribution of the time server is busy with transmission of the failed packets in every renewal from (3.42) as $O = \sum_{i=0}^{L}(W_i)$. From the derived relations in (3.57) and (3.48), the expected value of O is thus given by

$$\mathbb{E}[O] = \begin{cases} \frac{\varepsilon\varepsilon_N}{(1-\varepsilon)(1-\varepsilon(1-\varepsilon_N))} & \text{ARQ} \\ \frac{e^{\theta\varepsilon_N}}{\varepsilon_N}\left(1-e^{-\theta\varepsilon_N}(1+\varepsilon_N(1-\varepsilon_N)\theta)\right) & \text{HARQ} \end{cases} \tag{3.64}$$

Using the above computed relations for the terms C and O and the expression of $\mathbb{E}[X]$ in (3.59), the long term channel utilization, ($\overline{\eta}$), under non-preemptive policy can be expressed as

$$\overline{\eta} = \begin{cases} \frac{\lambda(1-\varepsilon_A)}{1-\lambda\varepsilon\varepsilon_A-(1-\lambda)(\varepsilon_A+\varepsilon(1-\varepsilon_N)(1-\varepsilon_A))} & \text{ARQ} \\ \frac{\lambda(1-e^{-\theta\varepsilon_N}(1-\varepsilon_N))}{\lambda+\varepsilon_N(1-\lambda)-e^{-\theta\varepsilon_N}\lambda(1-(\varepsilon_N+\varepsilon_N))} & \text{HARQ} \end{cases} \tag{3.65}$$

3.4 Analytical and Simulation Results

In this section, we present the AAoI analysis using both numerical and simulation results of the introduced system and compare the performance of the two queue management policies: preemptive and non-preemptive. We assume the value of $\rho = 0.75$ in (3.4) for both ARQ and HARQ protocols.

First, we show the impact of the SNR levels of the carried signal in the feedback channel on the average age performance in Fig. 3.3. Here, the performance of both ARQ and HARQ protocols are under study for an unreliable forward channel with SNr level of $\mathsf{snr}_d = -4$dB. We note first that the simulation results coincide with the numerical expressions attained in the previous sections for AAoI. First, at low load ($\lambda = 0.2$), the two preemptive and non-preemptive policies perform similarly and as the feedback channel quality improves (higher SNR), the average age, as expected, reduces. This is due to the fact that the feedback channel at higher SNR delivers more reliably the control messages (ACK/NACK), which allows for new samples to be transmitted and hence delivered to the monitor, ultimately decreasing the age. Now at a higher load (0.85), the performance is slightly different. For example, we first observe that for ARQ and under non-preemption, the age rather increases as we enhance the control channel quality. This is explained as follows. First, at a

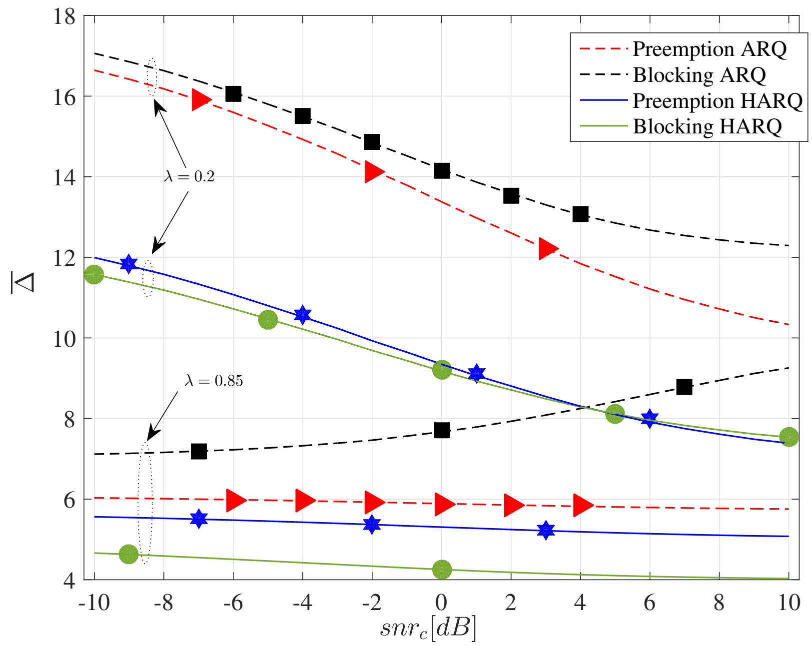

Figure 3.3: $\overline{\Delta}$ versus SNR in the feedback channel for a Symmetric Binary Channel model ($\Theta = 0$) and $\mathsf{snr}_d = -4$dB; Monte-Carlo simulations (markers) and analytical results (lines).

low SNR, the error probability on the control channel is higher, and hence the likelihood of miss-classification is higher. Given the low SNR on the forward channel, data packets will more likely be corrupted, and hence the monitor will be sending more often NACKs. If the feedback channel miss-classify these packets (which occur at a low snr_c), then chances of a NACK to be decoded as ACK is higher, and such ACK will admit a new sample to the sensor's buffer. Such new samples will remove old packets from the system, and hence yield the delivery of fresher samples which help in reducing the AAoI. On the other hand, at a higher snr_c, error in classification is getting lower and hence NACKs will be decoded more accurately. Such NACKs will block new samples from being admitted and the sensor spends more time transmitting the same packet in service. This results in increased age performance. However, the system under HARQ non-preemptive queue does not behave similarly, since re-transmissions enable HARQ in better delivering packets in service. Also, it should be noted that in the preemption policy, we do not have the same observation. Rather, since we are in the high load regime, newer samples are always admitted to remove old packets from the system and accordingly, the impact of the error in the feedback channel is negligible.

Next, we study the performance of the average AoI under different detection threshold (Θ)

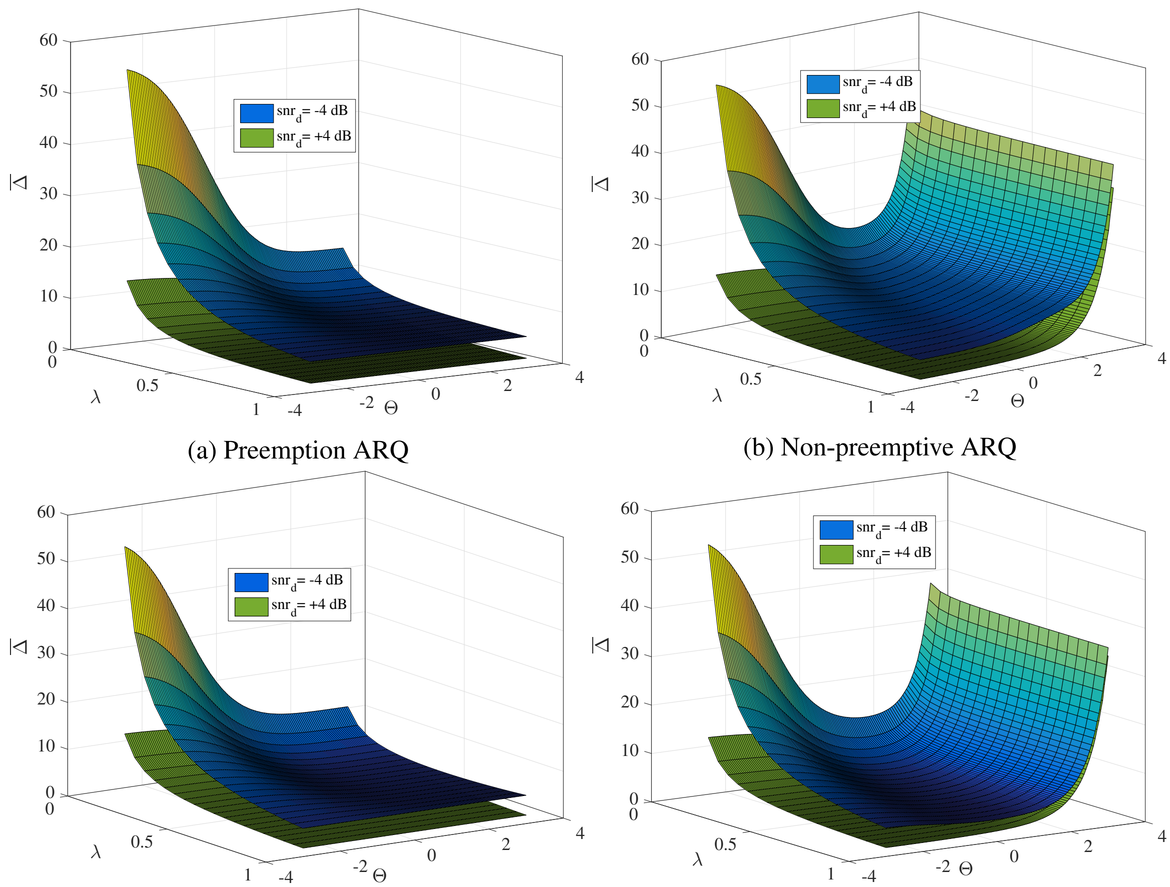

(a) Preemption ARQ

(b) Non-preemptive ARQ

(c) Preemption HARQ

(d) Non-preemptive HARQ

Figure 3.4: $\overline{\Delta}$ vs Θ levels and different packet generation rates (λ) for $\mathsf{snr}_c = 0$dB and $\mathsf{snr}_d = -4, +4$dB.

values in Fig. 3.4. This Figure shows the behavior of AAoI for high and low level of SNR values in forward channel ($\mathsf{snr}_d = +4, -4$dB) with a moderate SNR level in the feedback channel ($\mathsf{snr}_c = 0$dB). The analysis for the preemptive and non-preemptive policies are provided as follows.

(1) **preemptive policy:** Figs. (3.4(a)) and (3.4(c)) show the average age for both ARQ and HARQ under a preemption policy, by varying the rate of arrival of samples at the sensor and Θ. First, we observe that both ARQ and HARQ behave in a similar manner. Recall, that Θ serves as a classifier for the received messages at the sensor based on their signal strengths. When Θ is high, it becomes difficult to classify a received message as ACK, and irrespective of the outcome of decoding the signal at the monitor, more often the sensor is interpreting the received signals as NACKs, triggering the sensor to carry out re-transmissions. Now, when

the value of λ is low, the inter-arrival time of samples is high and therefore the sensor will be re-transmitting the same packet from its queue. This results in more frequent transmissions and hence reduce the average age at the monitor, as shown in Fig. (3.4(a)) (low λ and high Θ regime). However when Θ is low, the average AoI attain a higher value at low loads, since in this case, the sensor is more frequently classifying the received messages as ACKs and accordingly removing the packet under service from its buffer; however due to the large inter-arrival time, the buffer will be empty for sometime and the sensor transmission activity will be delayed, causing the large age increase at the monitor, as depicted by the Figure. On the other hand, when the load (λ) increases, a packet in service is continuously being preempted by the arriving samples at the sensor and therefore, the feedback channel does not play any major role since the delivery of either ACK or NACK becomes of no value to the sensor. This is evident from the figures where the value of Θ plays no meaningful role in the performance of the age metric.

(2) **non-preemptive policy:** Next, we present and analyse the results of the non-preemptive policy. We observe from Fig. (3.4(b)) and (3.4(d)) that both ARQ and HARQ behave similarly. However, the behavior of this non-preemptive policy differs than that of preemption. First, when the forward link experiences high loss rate (e.g., $\mathsf{snr}_d = -4$dB), more often the packets in service will arrive in errors at the monitor and as a result, NACK messages will be sent back on the backward channel. In the regime of (λ low/high and Θ high), ACK/NACK messages are often classified as NACKs, and that will trigger more re-transmissions of an old packet, blocking any new arriving packets from replacing the packet in service. This results in the large increase of AAoI in this regime. As a matter of fact, it should be noted that the arrival rate λ does not play any role, since even at a high rate of arrival, the new samples are blocked from being admitted into the sensor's buffer. Now, in the regime of (low λ and low Θ), most packets on the feedback channel are classified as ACKs (many incorrectly), after which the sensor removes the packet from its buffer until it receives a new packet to transmit (at low λ, inter-arrival is high, and hence the increase in age). As Θ slightly increases, we see a more robust classification which allows NACKs to be decoded correctly, triggering re-transmissions

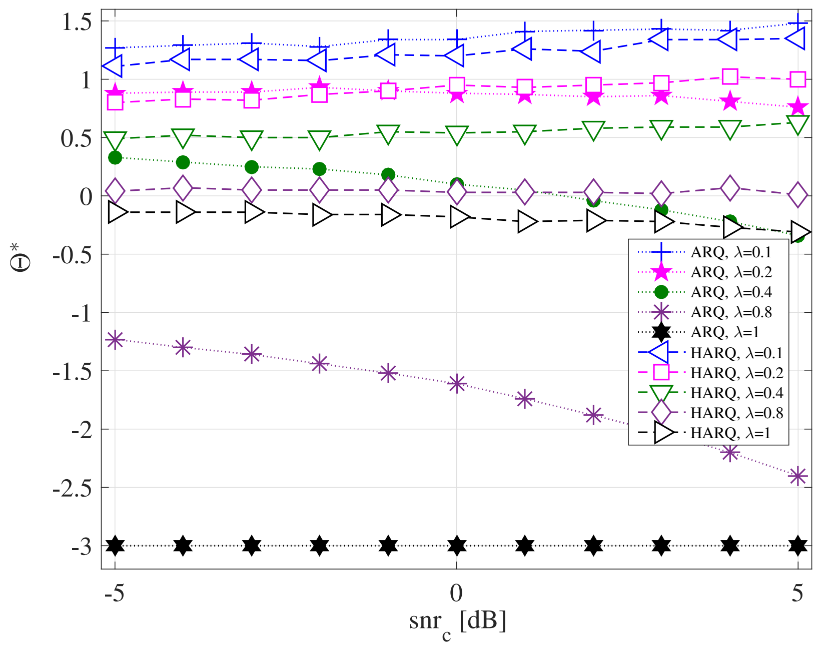

Figure 3.5: Optimum Θ for levels of SNR experienced in the feedback channel in a non-preemptive queue

by the sensor, after which the monitor successfully receives the packet. This manifests in the reduction of the AAoI in this regime. Finally, in the regime of (λ high, Θ low), we observe a lower attainable AAoI; in this regime, the classifier yields more ACKs than NACKs. An ACK message allows any new sample to be admitted and replace the packet in the queue. Particularly, at high λ, inter-arrival times of samples is low and thus the gain in the age performance. Last, when the quality of the forward channel is good ($\mathsf{snr}_c = +4$dB), the regime of (λ low, Θ low) results in lower age performance. In this case, messages transmitted by the sensor have high likelihood of being delivered successfully, and the monitor sends back more ACKs than NACKs. When Θ is low, the classification of ACK is done correctly, and hence emptying the sensor's buffer for a new arrival instead of blocking it. Indeed, reducing Θ indefinitely will cause the miss-classification of NACKs as ACKs, preventing the sensor from re-transmitting the packet in service. An increase in the age can be observed in this regime.

Optimal BAC model setup: As shown earlier, the performance of the average age is affected by the selected value of Θ, and hence for each configuration, an optimal value (Θ^*) which yields optimal system performance (lowest age) can be used to configure the system. In the case of a preemption,

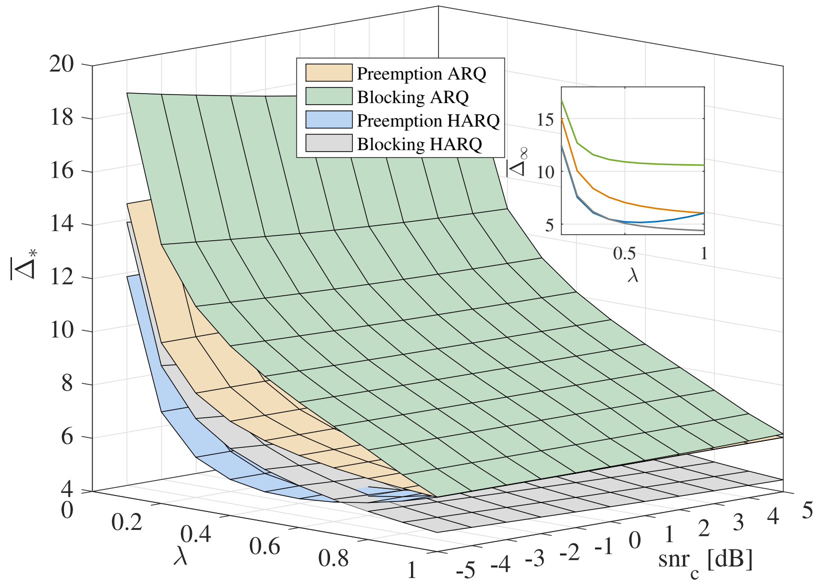

Figure 3.6: Optimum AAoI for $\mathsf{snr}_d = -4$ dB

it is clear that the higher the value of Θ, the lower the average age is, Remark 3.2.1 along with (3.35) provides the optimal average age for infinitely large Θ value. On the other hand, for the non-preemptive policy, neither a small nor a large value of Θ provides optimal system performance. In this policy, Θ^* is obtained through a linear search procedure. The optimal operational Θ is plotted vs. the feedback channel for some different traffic loads in Fig. 3.5. What is evident from the figure is that in general, the value of Θ^* remains constant for different system setups, however there is also a clear indication that in some channel realization (e.g., ARQ system with λ=0.8 or 0.4), the value of the Θ threshold that results in minimal age performance should change as the SNR of the control channel changes. The reason being that with lower Θ, the classifier at the sensor classifies messages more often as ACKs, this implies that (since the policy is non-preemptive), new packets are more often admitted to the system and they themselves help attain lower age performance. The reason this behavior is not shown for the load $\lambda = 1$, is because the system is already operating at a low enough value of Θ.

Fig. 3.6 shows the minimum achievable average AoI (using the obtained Θ^*) for different *snr* regimes in the feedback channel and packet generation rates (λ). It is trivial that the optimal Θ^* in the case of preemption can be attained for a positive infinite Θ. In Fig. 3.6, the value of Θ^* is set to 3, which shows to provide a worst case distance of 10^{-4} for the average age from the optimal average AoI value (from (3.35)) which is attained under the shown system setup. In the case of non-preemptive, the optimum value of Θ is calculated through a search method and some examples of it are shown in Fig. 3.5. In the figure, we show the behaviour of the management policies for ARQ and HARQ in case of an error-free feedback channel. First, it can be observed that the trend of changes under the optimal setup is the same of an error-free feedback channel and:

- In ARQ policy, preemption always performs better than non-preemptive queue: in case of ARQ scheme, since transmission of a new packet finds the same probability of success decoding as re-transmitting an old packet, preempting the service of the current packet and sending the new generated will lower the age more. Therefore, the optimum Θ value always tends to detect more reliably the ACK messages to avoid unnecessary re-transmissions that result in increasing the age due to missing the chance of transmitting more new and fresh packets. Therefore, we can observe in the figure that in any arrival rate $\lambda < 1$, the average age decreases with snr_c since not only the ACK miss-detection probability will be lower, but also the NACK miss-detection error can be set to a low value at the same time.

- In HARQ, non-preemptive policy can outperform the preemption if we have a more frequent packet arrival at the sensor. In higher packet arrival rates (higher value of λ), more status update packets are available in the buffer which can provide the chance for non-preemptive policy to lower its waiting time for accepting a new packet once emptying its buffer. Therefore, the average AoI will decrease monotonically under non-preemptive management. However, in preemptive queue, packets observe a lower chance to complete their re-transmissions due to the more events of preemption. Thus, the average AoI increases in this case. As a result, the non-preemptive might be a better approach for a system with a high rate of generating the status updates.

Importantly, we can observe that the minimum average age in case of non-preemptive policies can reach a lower level in comparison with an error-free feedback channel. Here, the miss-classification of NACK messages can provide a chance for newer packets to enter the system and be delivered to the monitor. Therefore, the age can decrease more since fresher packets are admitted. By controlling the value of Θ, we can lower the age by providing more chances for such

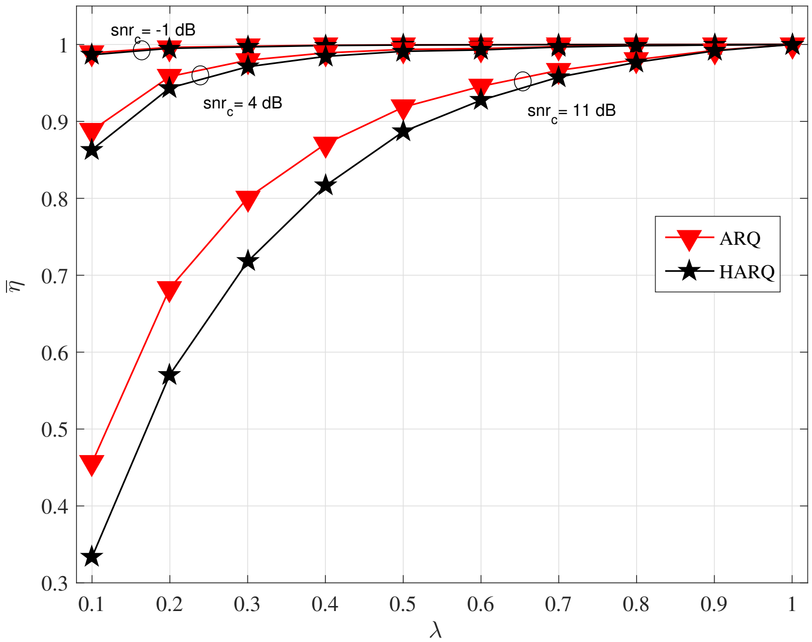

Figure 3.7: $\overline{\eta}$ versus λ (for Θ^*) for a system under a preemptive queue management.

newer packets to be served. Consequently, we can expect that the average optimum age under ARQ non-preemption performs the same as in preemption since the ACK messages can be detected more reliably than the NACK messages and hence more preemption will occur and the age reaches the same value in preemption ARQ.

Age/Channel Utilization trade-off: Our earlier study shows that under a preemptive policy, a blind re-transmission by the sensor without feedback messages can provide the same performance as in an error-free control channel model. However the cost of blind re-transmission manifests itself in conducting unnecessary re-transmission of status packets and utilizing fully the channel resources. To obtain a better insight into the effect of optimum design of control channel on the channel occupancy, we determine the lowest Θ value guaranteeing a certainty distance of 10^{-4} from the optimal average age value and we plot the channel utilization by varying arrival rate (λ) in Fig. 3.7. We can observe that with a poor control channel, the wireless channel is fully utilized under different λ values. However, with a strong control channel, a more reliable ACK/NACK detection can be designed through Θ^* which can reduce the utilization of the channel resources while maintaining the optimum average age ($\overline{\Delta}_*$).

Moreover, in the case of a non-preemptive policy, recall from Figs. (3.4(b)) and (3.4(d)) that at

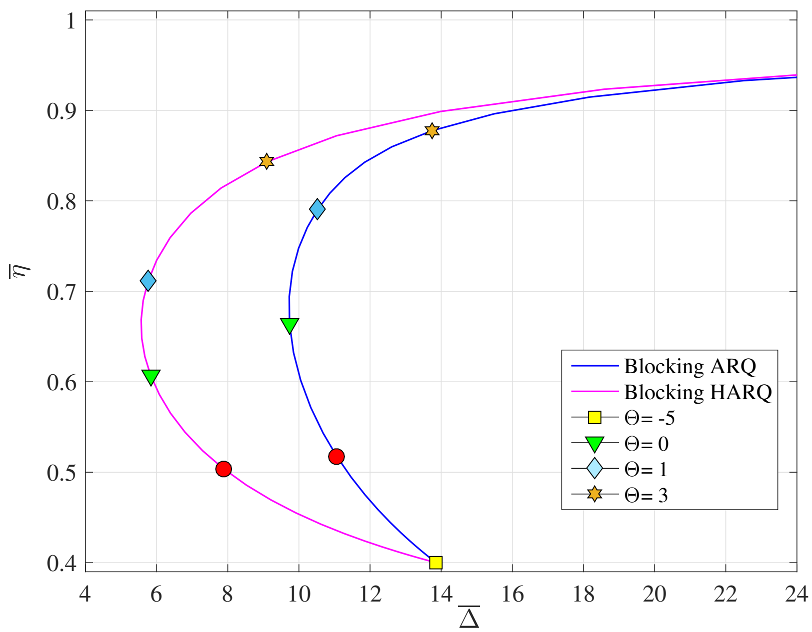

Figure 3.8: $\overline{\eta}$ versus $\overline{\Delta}$ for a non-preemptive system with ($\mathsf{snr}_c = 0$dB, $\mathsf{snr}_d = -4$dB and $\lambda = 0.4$); Monte-Carlo simulations (markers) and analytical results (lines).

lower arrival rates (λ), the average age plot is parabolic where we can attain the same average age value with two different setups of Θ levels. From the performance of AAoI, the two values of Θ are the same however from the channel resource utilization, indeed the lower Θ value might be preferred which can lower more the utilization of resources, as shown in Fig.3.8. Here, ACK messages are detected more reliably, and hence sensor will terminate the status packet re-transmissions faster which result in lowering the channel resource utilization than higher Θ values.

3.5 Conclusion

This chapter analyzed the performance of re-transmission protocols in terms of AAoI under a real practical noisy environment where the data and control wireless channels are prone to errors. Using the well-known model of packet combining schemes and binary detection strategy, we bridged the gap between the communication-theoretic error-prone control channel and the analysis of AAoI shown in the literature.

We derived the closed-form expressions of the average AoI for a real-time update system with preemptive and non-preemptive queue policies. We have shown that a noisy feedback channel increases the average AoI significantly in the absence of a proper ACK/NACK detection model. Throughout this study, we have seen that minimizing the average AoI requires designing the optimal parameter of the employed BAC model that takes into account the condition of both forward and feedback channels, the packet arrival process and the specific queue management policy. Simulations validated the theoretical analysis and showed that the preemptive queue is more sensitive to reliable NACK messages compared to the ACK signals, specially in high noisy feedback channel. Alternatively, the optimal parameter design of the control channel for non-preemptive queue revealed that the reliability in ACK/NACK signal detection may change with the packet arrival rate in the buffer, and hence the optimum design of feedback signalling is of most importance for this policy.

Further, our analysis revealed that the relationship between the non-preemptive and preemptive policies depends on the operational SNR and the parameter of detection channel model. In particular, for low SNR, where decoding errors are frequent and the value of using HARQ most significant, the non-preemptive is preferable over the preemption under the optimum detection parameter setup. While we address the issue of AoI in imperfect wireless channel setup with fixed preemptive and non-preemptive policies, there still remain rooms for further analysis of deploying a controller on the sensor to make dynamic packet transmissions to enhance the AoI performance.

Chapter 4

Conclusion and Future Work

In this thesis, we investigated two issues in the semantic communication systems. In the first part, we argued that semantic communication is not limited to the real-time applications, and accordingly we proposed the semantic communication for non-real time systems. Further, we studied the systems under re-transmission schemes to mitigate the impact of unreliability imposed in the wireless channel in practice. The analysis showed that the optimal policies of a causal system can not be optimal in a non-causal system. In particular, we showed that a system operating under a powerful packet combining strategy such as HARQ will always perform better under the fixed blocking policy in terms of information accuracy. However, in a more simple packet combining strategy such as ARQ, both fixed preemption and blocking policies provide the same performance in terms of information accuracy. Moreover, we indicated that the non-causal estimation is more robust in presence of the model mismatch, and thus might be preferred in applications with less stringer constraints on the delivery time.

Formulating the concept of timeliness as a measurement of Information Semantic still remains as an open issue to solve. The timeliness must be reformulated and revisited considering the user service demand as proposed in the Semantic of Information. In this direction, a possible future work might be to formulate the concept of timeliness in non-real time systems. Moreover, we assumed Gaussian Markov processes in this work which can be further generalized to more complex processes. To enable more intelligent networks, the source model can be assumed as an unknown source and the Semantics can be further designed by implementing Machine Learning techniques.

The second part of the work investigated the issue of the feedback unreliability in real-time sensor networks. It was shown that the assumption of error-free feedback channel can significantly reduce the performance of the Age of Information in a practical environment. Accordingly, we applied a Binary Asymmetric Channel in the control channel to discover the errors in the feedback signal. The numerical results and analysis provided detailed perspectives on the optimal BAC setup minimizing the average AoI and the possible trade-off between AoI and resource utilization. Generally, the analysis for a preemption setting illustrated that a better protection for the NACK messages compared to the ACK messages can preserve the minimum AoI performance. Specially, under a high noisy feedback channel setup, we showed that the viable solution minimizing the average AoI is a blind transmission mechanism at the cost of increasing unnecessary utilization of the channel resources. Moreover, the analysis for a non-preemptive queue revealed the dependence of the optimal BAC design on the status packet generation rate at the sensor. Such a dependency makes the BAC model to provide a more reliable ACK detection compared to NACK messages under the condition of more frequent packet arrival, whereas the opposite holds under the condition of less frequent packet arrival.

In future works, we can implement more intelligent feedback signal detection and correction by adopting Machine Learning techniques. Also, other types of re-transmission schemes such as Incremental Redundancy Hybrid Automatic Repeat Request which is widely used in 5G systems can be implemented in real-time systems and the impact of errors with this scheme can be studied. Moreover, we assumed a single user scenario in this dissertation which can be further extended to the multi-user scenarios with multi-casting or broad-casting packet communication.

Appendix A

Denoting by L the random number of preempted packets, the time the sensor is busy with their transmission is given by $F = \sum_{i=0}^{L} A_i$, where A_i are independent, identically distributed (i.i.d.) and model the transmission time of the i-th preempted packet.

To find F, we need to calculate the distribution of L and A_i. First, starting with calculation of probability distribution for L quantifying the number of preempted packets. Considering p as the probability that a packet under service is not preempted, we will have

$$p = \Pr\{S \leq R\} = \begin{cases} \frac{1-\varepsilon}{1-\varepsilon(1-\lambda)} & \text{ARQ} \\ \exp(-\theta\lambda) & \text{HARQ} \end{cases} \tag{A.1}$$

Since each packet is preempted independently with probability $1-p$, and L is their total number, we have $L \sim \text{Geom}(p)$, which immediately yields its PGF $G_L(z) = \frac{p}{1-(1-p)z}$.

As for $A = A_i$, which is the inter-arrival time between two consecutive packets conditioned on the first being preempted, we find its distribution as[1]

$$\Pr\{A = k\} = \Pr\{R = k | S > R\} = \frac{\Pr\{R = k \wedge S \leq k\}}{\Pr\{S \leq R\}} = \begin{cases} \frac{(1-\lambda)^{k-1}\lambda\varepsilon^k}{1-p} & \text{ARQ} \\ \frac{(1-\lambda)^{k-1}\lambda \mathrm{e}^{-\theta} r_k(\theta)}{1-p} & \text{HARQ} \end{cases} \tag{A.3}$$

[1] All calculations are done by the explicit summations over the arguments of the distribution. For example, to calculate (A.1) we plug (2.8) and (2.3) in

$$\Pr\{S \leq R\} = \sum_{s=1}^{\infty} \sum_{r=s}^{\infty} \Pr\{S = s\} \Pr\{R = r\}; \tag{A.2}$$

changing the order of summations simplifies the algebra and yields (A.1).

where, $r_k(\theta) = \mathrm{e}^{\theta} - \sum_{t=0}^{k} \frac{\theta^t}{t!}$, and then its probability generating function

$$G_A(z) = \mathbb{E}[z^A] = \sum_{k=1}^{\infty} z^k Pr\{A = k\} = \begin{cases} \frac{z(1-\varepsilon(1-\lambda))}{1-z(1-\lambda)\varepsilon} & \text{ARQ} \\ \frac{\lambda z(1-\mathrm{e}^{-\theta(1-(1-\lambda)z)})}{(1-p)(1-(1-\lambda)z)} & \text{HARQ} \end{cases} \tag{A.4}$$

Now, we compute the PGF of F via Wald's equality [49, Theorem 3.3.2]

$$G_F(z) = G_L(G_A(z)) = \begin{cases} \frac{(1-\varepsilon)(1-z(1-\lambda)\varepsilon)}{(1-\varepsilon(1-\lambda))(1-z\varepsilon)} & \text{ARQ} \\ \frac{\mathrm{e}^{-\theta\lambda}(1-(1-\lambda)z)}{1-z(1-\lambda\mathrm{e}^{-\theta(1-(1-\lambda)z)})} & \text{HARQ} \end{cases} \tag{A.5}$$

Appendix B

To calculate $\mathbb{E}[X\mathrm{e}^{-2n\alpha X}]$, we need to take into account the definition of X through (2.52). The defined relation in expectation by considering the independence between I, F and Y can be formulated as the following

$$\begin{aligned}\mathbb{E}[X\mathrm{e}^{-2n\alpha X}] = &\mathbb{E}[I\mathrm{e}^{-2n\alpha I}]\,\mathbb{E}[\mathrm{e}^{-2n\alpha F}]\,\mathbb{E}[\mathrm{e}^{-2n\alpha Y}] + \mathbb{E}[F\mathrm{e}^{-2n\alpha F}]\,\mathbb{E}[\mathrm{e}^{-2n\alpha I}]\,\mathbb{E}[\mathrm{e}^{-2n\alpha Y}] \\ &+ \mathbb{E}[Y\mathrm{e}^{-2n\alpha Y}]\,\mathbb{E}[\mathrm{e}^{-2n\alpha I}]\,\mathbb{E}[\mathrm{e}^{-2n\alpha F}]\end{aligned} \tag{B.1}$$

From (2.53), we can find the expectation of $I\mathrm{e}^{-2n\alpha I}$

$$\mathbb{E}[I\mathrm{e}^{-2n\alpha I}] = \frac{\lambda \mathrm{e}^{-2n\alpha}}{(1-(1-\lambda)\mathrm{e}^{-2n\alpha})^2} \tag{B.2}$$

Next, for calculating the expectation of $Fe^{-2n\alpha F}$, we can apply the Wald's equality

$$\begin{aligned}\mathbb{E}[F\mathrm{e}^{-2n\alpha F}] &= \sum_{l=0}^{\infty} l\,\mathbb{E}[\mathrm{e}^{-2An\alpha}]^{l-1}\,\mathbb{E}[A\mathrm{e}^{-2An\alpha}]P_L(l) = \frac{p(1-p)\,\mathbb{E}[A\mathrm{e}^{-2n\alpha A}]}{(1-(1-p)\,\mathbb{E}[\mathrm{e}^{-2n\alpha A}])^2} \\ &= \begin{cases} \frac{\varepsilon\lambda(1-\varepsilon)\mathrm{e}^{-2n\alpha}}{(1-\varepsilon(1-\lambda))(1-\varepsilon\mathrm{e}^{-2n\alpha})^2} & \text{ARQ} \\ \frac{Q_n\lambda\mathrm{e}^{-\theta(1+\lambda)}(\mathrm{e}^{\theta}-\mathrm{e}^{Q_n\theta}(1+Q_n(1-Q_n)\theta))}{(1-\lambda)(1-Q_n-\lambda\mathrm{e}^{-2n\alpha}(1-\mathrm{e}^{-\theta(1-Q_n)}))^2} & \text{HARQ} \end{cases}.\end{aligned} \tag{B.3}$$

In which the expectation of $Ae^{-2n\alpha A}$ can be calculated from (A.4)

$$\mathbb{E}[A\mathrm{e}^{-2n\alpha A}] = \begin{cases} \frac{(1-\varepsilon(1-\lambda))\mathrm{e}^{-2\alpha n}}{(1-\varepsilon(1-\lambda)\mathrm{e}^{-2\alpha n})^2} & \text{ARQ} \\ \frac{Q_n\lambda\mathrm{e}^{-\theta}(\mathrm{e}^{\theta}-\mathrm{e}^{Q\theta}(1+Q_n\theta(1-Q_n)))}{(1-\mathrm{e}^{-\theta\lambda})(1-\lambda)(1-Q_n)^2} & \text{HARQ} \end{cases}, \tag{B.4}$$

where

$$Q_n = (1-\lambda)\mathrm{e}^{-2n\alpha} \tag{B.5}$$

From the above equations and (2.54), (2.58), (2.53), after some simplifications, we obtain

$$\mathbb{E}[X\mathrm{e}^{-2n\alpha X}] = \begin{cases} \frac{\lambda(1-\varepsilon)\mathrm{e}^{-2n\alpha}(1-\varepsilon(1-\lambda)\mathrm{e}^{-4n\alpha})}{(1-(1-\lambda)\mathrm{e}^{-2n\alpha})^2(1-\varepsilon\mathrm{e}^{-2n\alpha})^2} & \text{ARQ} \\ \frac{\lambda Q_n \mathrm{e}^{-\theta(1+\lambda)}U}{(1-\lambda)(1-Q_n)} & \text{HARQ} \end{cases}, \tag{B.6}$$

where

$$U = \frac{\lambda\mathrm{e}^{-\theta(1-\lambda)(1-\mathrm{e}^{-2n\alpha})-2n\alpha}(\mathrm{e}^{\theta}-(1+Q_n(1-Q_n)\theta\mathrm{e}^{Q_n\theta}))}{(1-Q_n-\lambda\mathrm{e}^{-2\alpha}(1-\mathrm{e}^{-\theta(1-Q_n)}))^2} + \frac{\mathrm{e}^{\theta(Q_n+\lambda)}(1+\theta Q_n(1-Q_n))}{(1-\mathrm{e}^{-2n\alpha}(1-\lambda\mathrm{e}^{-\theta(1-Q_n)}))} \tag{B.7}$$

Appendix C

We compute $\mathbb{E}[Xe^{-2n\alpha X}]$ from the following relation by considering the equation in (3.42)

$$\mathbb{E}[X\mathrm{e}^{-2n\alpha X}] = \mathbb{E}[I\mathrm{e}^{-2n\alpha I}]\,\mathbb{E}[\mathrm{e}^{-2n\alpha S}] + \mathbb{E}[S\mathrm{e}^{-2n\alpha S}]\,\mathbb{E}[\mathrm{e}^{-2n\alpha I}] \tag{C.1}$$

From (2.8), we have:

$$\mathbb{E}[\mathrm{e}^{-2\alpha S}] = \begin{cases} \frac{\mathrm{e}^{-2\alpha}(1-\varepsilon)}{1-\varepsilon\mathrm{e}^{-2\alpha}} & \text{ARQ} \\ \mathrm{e}^{-\theta(1-\mathrm{e}^{-2\alpha})-2\alpha} & \text{HARQ,} \end{cases} \tag{C.2}$$

$$\mathbb{E}[S\mathrm{e}^{-2\alpha S}] = \begin{cases} \frac{\mathrm{e}^{-2\alpha}(1-\varepsilon)}{(1-\varepsilon\mathrm{e}^{-2\alpha})^2} & \text{ARQ} \\ \mathrm{e}^{-\theta(1-\mathrm{e}^{-2\alpha})-2\alpha}(1+\theta\mathrm{e}^{-2\alpha}) & \text{HARQ} \end{cases}. \tag{C.3}$$

From the above equations and (B.2), we can obtain

$$\mathbb{E}[X\mathrm{e}^{-2n\alpha X}] = \begin{cases} \frac{\lambda(1-\varepsilon)\mathrm{e}^{-2\alpha}(1-\varepsilon(1-\lambda)\mathrm{e}^{-4\alpha})}{(1-(1-\lambda)\mathrm{e}^{-2\alpha})^2(1-\varepsilon\mathrm{e}^{-2\alpha})^2} & \text{ARQ} \\ \frac{\lambda\mathrm{e}^{-\theta(1-\mathrm{e}^{-2\alpha})-2\alpha}(2+(1-Q_n)(1+\theta\mathrm{e}^{-2\alpha}))}{(1-(1-\lambda)\mathrm{e}^{-2\alpha})^2} & \text{HARQ} \end{cases}, \tag{C.4}$$

where Q_n is given by (B.5).

Appendix D

With our formulation of the MDP process, the action a_t we take has the potential of affecting the cost at future renewals, that is, at the arrival of the packet currently being serviced which we index with $\check{m}$ so the corresponding cost is obtained from (2.42) as

$$C_{\check{m}} = \frac{1}{2}((X_{\check{m}} + Y_{\check{m}})^2 - Y_{\check{m}}^2). \tag{D.1}$$

Similarly, the cost of the next renewal is given by

$$C_{\check{m}+1} = \frac{1}{2}((X_{\check{m}+1} + Y_{\check{m}+1})^2 - Y_{\check{m}+1}^2). \tag{D.2}$$

We need to find the action prior to the renewal, that is $a_t, t < D_{\check{m}}$, which minimizes the sum $C_{\check{m}} + C_{\check{m}+1}$ so we need to determine which elements of (D.1) and (D.2) are affected by a_t; to this end we make the following observations:

- In ARQ, the probability of successfully delivering a packet at each time slot is equal to $(1-\varepsilon)$, see (2.79); it is thus independent of the action $a_t, t < D_{\check{m}}$. Consequently, $D_{\check{m}}$ is not affected by a_t and neither is $(X_{\check{m}} + Y_{\check{m}})$.
- The value of $Y_{\check{m}+1}$ is only affected by the decisions made at renewal $\check{m}+1$ and not by $a_t, t < D_{\check{m}}$.
- Setting $X_{\check{m}+1} = Y_{\check{m}} + Z_{\check{m}+1}$, where $Z_{\check{m}+1} = B_{\check{m}+1} - D_{\check{m}}$, we note that $Z_{\check{m}+1}$ is not affected by a_t.

- The decision $a_t, t < D_{\check{m}}$ affects the value of $Y_{\check{m}}$: it is decreased by the preemption, $a_t = 1$, and increased by the blocking, $a_t = 0$.

We can thus write

$$C_{\check{m}} + C_{\check{m}+1} = \text{Const.} + Y_{\check{m}}(Z_{\check{m}+1} + Y_{\check{m}+1}), \tag{D.3}$$

where Const. contains all the terms independent of the action a_t. Since $Z_{\check{m}+1}$ and $Y_{\check{m}+1}$ are independent of a_t and $Y_{\check{m}}$ is minimized by $a_t = 1$, the preemption minimizes the cost.

Appendix E

Recall from the policy in a preemptive queue that a packet under service may be preempted by another packet and leave the system before completing its transmissions. Therefore, the time a packet consumes from the system until a preemption event terminated its service will be equal to the inter-generation time of two successive packets provided that the first stays in the service once a new one arrives the queue. Hence, from the independence of status packet generation and feedback events, we can have the following relation for time duration A

$$\begin{aligned}\mathbb{P}_A(k) &= \Pr\{R = k | \{S > R\}, \{\hat{D}_{1:R} = N | D_{1:R} = N\}\} \\ &= \frac{1}{P_\Psi} \mathbb{P}_R(k) \sum_{j=k}^{\infty} \mathbb{P}_S(j) \prod_{i=1}^{k} \mathbb{P}(\hat{D}_i = N | D_i = N)\end{aligned} \tag{E.1}$$

Next, we compute the duration of dropped packets due to NACK detection errors, defined by B. B indicates the number of time slots elapsed to detect a NACK feedback as ACK for the first time, as long as no new update packet interrupts its transmissions. Therefore, the probability distribution of variable B is:

$$\begin{aligned}\mathbb{P}_B(k) &= \Pr\{F = k | \{R \geq F\}, \{\hat{D}_{1:F-1} = N, \hat{D}_F = A | D_{1:F} = N\}\} \\ &= \frac{1}{P_\Upsilon} \mathbb{P}_F(k) \{\mathbb{P}(R \geq k) \mathbb{P}(\hat{D}_{1:k-1} = N, \hat{D}_k = A | D_{1:k} = N)\}\end{aligned} \tag{E.2}$$

Due to the relation of $\mathbb{P}_F(k) = \sum_{i=k+1}^{\infty} \mathbb{P}_S(i)$ in both ARQ and HARQ re-transmission schemes, we can show the equality of the probability distributions of A and B. Further, the distribution can be evaluated as

$$\mathbb{P}_A(k) = \mathbb{P}_B(k) = \begin{cases} (1-\varepsilon(1-\varepsilon_N)(1-\lambda))(\varepsilon(1-\varepsilon_N)(1-\lambda))^{k-1} & \text{ARQ} \\ \frac{1-(1-\varepsilon_N)(1-\lambda)}{1-e^{-\theta(1-(1-\lambda)(1-\varepsilon_N)}}\gamma(\theta,w)((1-\varepsilon_N)(1-\lambda))^{w-1} & \text{HARQ} \end{cases} \tag{E.3}$$

Bibliography

[1] E. Altman, R. El-Azouzi, D. S. Menasche, and Y. Xu, "Forever young: Aging control for hybrid networks," in *Proc., Twentieth ACM International Symposium on Mobile Ad Hoc Networking and Computing*, 2019, pp. 91–100.

[2] A. Sciarretta, L. Guzzella, and M. Back, "A real-time optimal control strategy for parallel hybrid vehicles with on-board estimation of the control parameters," *IFAC Proceedings Volumes*, vol. 37, no. 22, pp. 489 – 494, 2004.

[3] H. B. Glasgow and et.al., "Real-time remote monitoring of water quality: a review of current applications, and advancements in sensor, telemetry, and computing technologies," *Journal of Experimental Marine Biology and Ecology*, 2004.

[4] M. Kountouris and N. Pappas, "Semantics-empowered communication for networked intelligent systems," *IEEE Communications Magazine*, vol. 59, no. 6, pp. 96–102, 2021.

[5] E. Uysal, O. Kaya, A. Ephremides, J. Gross, M. Codreanu, P. Popovski, M. Assaad, G. Liva, A. Munari, T. Soleymani, B. Soret, and K. H. Johansson, "Semantic communications in networked systems," *arXiv preprint arXiv:2103.05391*, 2021.

[6] R. D. Yates and S. K. Kaul, "Status updates over unreliable multiaccess channels," in *IEEE Inter. Symp. Inf. Theory (ISIT)*, June 2017, pp. 331–335.

[7] A. Kosta, N. Pappas, A. Ephremides, and V. Angelakis, "The cost of delay in status updates and their value: Non-linear ageing," *IEEE Trans. Commun.*, vol. 68, no. 8, pp. 4905–4918, 2020.

[8] A. Maatouk, M. Assaad, and A. Ephremides, “The Age of Incorrect Information: an Enabler of Semantics-Empowered Communication,” *CoRR*, vol. abs/2012.13214, 2020. [Online]. Available: https://arxiv.org/abs/2012.13214

[9] R. D. Yates, Y. Sun, D. R. Brown, S. K. Kaul, E. Modiano, and S. Ulukus, “Age of Information: An Introduction and Survey,” vol. 39, no. 5, pp. 1183–1210, 2021.

[10] A. Maatouk, S. Kriouile, M. Assaad, and A. Ephremides, “The Age of Incorrect Information: A New Performance Metric for Status Updates,” *IEEE/ACM Transactions on Networking*, vol. 28, no. 5, pp. 2215–2228, 2020.

[11] X. Zheng, S. Zhou, and Z. Niu, “Urgency of Information for Context-Aware Timely Status Updates in Remote Control Systems,” *IEEE Transactions on Wireless Communications*, vol. 19, no. 11, pp. 7237–7250, 2020.

[12] E. Najm and et.al., “Status updates through M/G/1/1 queues with HARQ,” in *IEEE Inter. Symp. Inf. Theory (ISIT)*, 2017.

[13] E. T. Ceran, D. Gündüz, and A. György, “Average Age of Information with Hybrid ARQ under a resource constraint,” *IEEE Transactions on Wireless Communications*, vol. 18, no. 3, pp. 1900–1913, 2019.

[14] R. Cam and C. Leung, “Throughput analysis of some ARQ protocols in the presence of feedback errors,” *IEEE Transactions on Communications*, vol. 45, no. 1, pp. 35–44, 1997.

[15] Y. Sun and B. Cyr, “Information aging through queues: A mutual information perspective,” in *2018 IEEE 19th International Workshop on Signal Processing Advances in Wireless Communications (SPAWC)*, 2018, pp. 1–5.

[16] S. Feng and J. Yang, “Information freshness for timely detection of status changes,” in *2020 54th Annual Conference on Information Sciences and Systems (CISS)*. IEEE, 2020, pp. 1–6.

[17] M. Wang, W. Chen, and A. Ephremides, “Real-time reconstruction of a counting process through first-come-first-serve queue systems,” *IEEE Transactions on Information Theory*, vol. 66, no. 7, pp. 4547–4562, 2020.

[18] T. Z. Ornee and Y. Sun, "Sampling for Remote Estimation through Queues: Age of Information and Beyond," in *(WiOPT)*, 2019, pp. 1–8.

[19] Y. Sun, Y. Polyanskiy, and E. Uysal-Biyikoglu, "Remote estimation of the Wiener process over a channel with random delay," in *IEEE Inter. Symp. Inf. Theory (ISIT)*, June 2017, pp. 321–325.

[20] Y. Sun and B. Cyr, "Sampling for data freshness optimization: Non-linear age functions," *Journal of Communications and Networks*, vol. 21, no. 3, pp. 204–219, 2019.

[21] M. Klugel, M. H. Mamduhi, S. Hirche, and W. Kellerer, "AoI-Penalty Minimization for Networked Control Systems with Packet Loss," in *IEEE INFOCOM 2019*, 2019.

[22] O. Ayan, M. Vilgelm, and W. Kellerer, "Optimal scheduling for discounted age penalty minimization in multi-loop networked control," *CCNC*, pp. 1–7, 2020.

[23] Y. Gu, H. Chen, Y. Zhou, Y. Li, and B. Vucetic, "Timely status update in Internet of Things monitoring systems: An age-energy tradeoff," *IEEE Internet of Things Journal*, vol. 6, no. 3, pp. 5324–5335, 2019.

[24] R. Devassy, G. Durisi, G. C. Ferrante, O. Simeone, and E. Uysal, "Reliable Transmission of Short Packets Through Queues and Noisy Channels Under Latency and Peak-Age Violation Guarantees," *IEEE J. Sel. Areas Commun.*, April 2019.

[25] S. K. Kaul, R. D. Yates, and M. Gruteser, "Status updates through queues," in *CISS*, March 2012, pp. 1–6.

[26] Y. Inoue, H. Masuyama, T. Takine, and T. Tanaka, "A General Formula for the Stationary Distribution of the age-of-information and Its Application to Single-Server Queues," *IEEE Trans. Inf. Theory*, Dec 2019.

[27] M. Costa, M. Codreanu, and A. Ephremides, "Age of information with packet management," in *IEEE Inter. Symp. Inf. Theory (ISIT)*, June 2014, pp. 1583–1587.

[28] P. D. Mankar, M. A. Abd-Elmagid, and H. S. Dhillon, “Spatial distribution of the mean peak Age of Information in wireless networks,” *IEEE Transactions on Wireless Communications*, 2021.

[29] A. Soysal and S. Ulukus, “Age of information in G/G/1/1 systems,” in *2019 53rd Asilomar Conference on Signals, Systems, and Computers*. IEEE, 2019, pp. 2022–2027.

[30] V. Tripathi, R. Talak, and E. Modiano, “Age of information for discrete time queues,” *arXiv preprint arXiv:1901.10463*, 2019.

[31] Y. Inoue, H. Masuyama, T. Takine, and T. Tanaka, “The stationary distribution of the age of information in fcfs single-server queues,” in *2017 IEEE International Symposium on Information Theory (ISIT)*. IEEE, 2017, pp. 571–575.

[32] K. Huang, W. Liu, M. Shirvanimoghaddam, Y. Li, and B. Vucetic, “Real-Time Remote Estimation with Hybrid ARQ in Wireless Networked Control,” *ArXiv*, vol. abs/1903.12472, 2019.

[33] J. Östman, R. Devassy, G. Durisi, and E. G. Ström, “Short-packet transmission via variable-length codes in the presence of noisy stop feedback,” *IEEE Transactions on Wireless Communications*, 2020.

[34] S. Marcille, P. Ciblat, and C. Le Martret, “Hybrid ARQ with Unreliable Feedback Channel.”

[35] M. W. El Bahri, H. Boujemaa, and M. Siala, “Effects of noisy feedback on the performance of HARQ schemes over multipath block fading channels for DS-SSS,” in *2005 IEEE 16th International Symposium on Personal, Indoor and Mobile Radio Communications*, vol. 4. IEEE, 2005, pp. 2552–2556.

[36] B. Makki, A. Graell i Amat, and T. Eriksson, “On Noisy ARQ in Block-Fading Channels,” *IEEE Transactions on Vehicular Technology*, vol. 63, no. 2, pp. 731–746, 2014.

[37] H. Shariatmadari, R. Duan, S. Iraji, R. Jantti, Z. Li, and M. A. Uusitalo, “Asymmetric ACK/NACK Detection for Ultra Reliable Low Latency Communications,” in *2018 European Conference on Networks and Communications (EuCNC)*, 2018, pp. 1–166.

[38] E. Malkamaki and H. Leib, "Performance of truncated type-II hybrid ARQ schemes with noisy feedback over block fading channels," *IEEE Transactions on Communications*, vol. 48, no. 9, pp. 1477–1487, 2000.

[39] H. Boujemâa, "Delays analysis of cooperative truncated HARQ with opportunistic relaying and noisy feedback," in *21st Annual IEEE International Symposium on Personal, Indoor and Mobile Radio Communications*. IEEE, 2010, pp. 1179–1183.

[40] T. Breddermann, B. Eschbach, and P. Vary, "Influence of HARQ with Unreliable Feedback on the Throughput of UMTS LTE," in *2012 IEEE Vehicular Technology Conference (VTC Fall)*. IEEE, 2012, pp. 1–5.

[41] H. Boujemâa, "Performance of truncated hybrid ARQ schemes with noisy feedback for DS-CDMA systems," *European transactions on telecommunications*, vol. 21, no. 4, pp. 375–385, 2010.

[42] M. Kountouris and N. Pappas, "Semantics-empowered communication for networked intelligent systems," *CoRR*, vol. abs/2007.11579, 2020. [Online]. Available: https://arxiv.org/abs/2007.11579

[43] P. Larsson, L. K. Rasmussen, and M. Skoglund, "Throughput analysis of ARQ schemes in Gaussian block fading channels," *IEEE Trans. Commun.*, vol. 62, no. 7, pp. 2569–2588, 2014.

[44] R. Sassioui, M. Jabi, L. Szczecinski, L. B. Le, M. Benjillali, and B. Pelletier, "HARQ and AMC: Friends or foes?" *IEEE Trans. Commun.*, vol. 65, no. 2, pp. 635–650, Feb. 2017.

[45] A. Kosta, N. Pappas, A. Ephremides, and V. Angelakis, "Age and value of information: Non-linear age case," in *2017 IEEE International Symposium on Information Theory (ISIT)*, 2017, pp. 326–330.

[46] G. Lindgren, *Stationary stochastic processes: theory and applications*. CRC Press, 2012.

[47] R. W. Wolff, *Stochastic modeling and the theory of queues*. Pearson College Division, 1989.

[48] S. Asvadi, S. Fardi, and F. Ashtiani, “Analysis of Peak Age of Information in Blocking and Preemptive Queueing Policies in a HARQ-Based Wireless Link,” *IEEE Wireless Communications Letters*, vol. 9, no. 9, pp. 1338–1341, 2020.

[49] S. Ross, *Stochastic Processes*. Wiley, 1995.